Aggravation of inflammation-induced encephalopathy by reduced ambient temperature –

Role of phosphoinositide 3-kinase gamma

Dissertation

To Fulfill the
Requirements for the Degree of
„Doctor of Philosophy" (PhD)

Submitted to the Council of the Faculty
of Biological Sciences
of the Friedrich Schiller University Jena

by M.SC. Lang, Guang-Ping

born on 03.12.1987 in Heilongjiang, China

Contents

Index of figures

Index of tables

List of abbreviations

5'-AMP	5'-Adenosine monophosphate
ACTH	adrenocorticotropic hormone
BBB	blood-brain barrier
cAMP	cyclic adenosine monophosphate
CNS	central nervous system
CVOs	circumventricular organs
DHCA	deep hypothermic circulatory arrest
DMEM	Dulbecco's Modified Eagle's medium
EB	Evans blue
ECAR	extracellular acidification rate
ECG	electrocardiography
ECs	endothelial cells
ERK	extracellular-signal-regulated kinase
FCS	fetal calf serum
FITC	Fluorescein isothiocyanate
FOXO	forkhead-box-protein O
GABA	gamma-aminobutyric acid
GAPDH	glyceraldehyde 3-phosphate dehydrogenase
GPCR	G protein coupled receptors
GSKβ	glycogen synthase kinase 3 beta
HR	heart rate
IL-1β	interleukin-1β
KD	kinase dead
KO	knock out
LCT	lower critical temperature
LPS	Lipopolysaccharides
MAPK	mitogen-activated protein kinase
MCP-1	monocyte chemoattractant protein 1
MEK	mitogen-activated protein kinase kinase
MMPs	matrix metalloproteinases
MOD	multiple organ dysfunction
NO	nitric oxide
NOS	nitric oxide synthase

NVU	neurovascular unit
OCR	oxygen consumption rate
PAMPs	pathogen-associated molecular patterns
PBS	phosphate-buffered saline
PDE3B	phosphodiesterase 3B
PDK1	phosphoinositide-dependent kinase 1
PFA	paraformaldehyde
PH	pleckstrin-homology
PI3Kγ	phosphoinositide 3-kinase γ
PIP	phosphatidylinositol 3-phosphate
PIP$_2$	phosphatidylinositol-3,4-bisphosphate
PIP$_3$	phosphatidylinositol-3,4,5-trisphosphate
PKA	protein kinase A
PKB	protein kinase B
POA	preoptic area
PRRs	pattern recognition receptors
PTEN	phosphatase and tensin homolog
qSOFA	quick Sequential Organ Failure Assessment
ROS	reactive oxygen species
RTKs	receptor tyrosine kinases
SAE	sepsis-associated encephalopathy
SH2	src homology 2
SIRS	systemic inflammatory response syndrome
T$_a$	ambient temperature
T$_c$	core body temperature
T$_{Inc}$	incubation temperature
TLRs	toll-like receptors
TNFα	tumor necrosis factor-alpha
TNZ	thermoneutral zone
TUNEL	terminal deoxynucleotidyl transferase dUTP nick end labeling

Summary

Sepsis-associated encephalopathy (SAE) is the most common form of encephalopathy occurring in critical care settings and refers to acute neurological dysfunction that arises in the context of extracranial sepsis. SAE is an early feature of infection in the body, occurs quite often with a prevalence of up to 30% in septicemic patients at admission and SAE severity is associated with increased mortality of septic patients. Although the symptoms of SAE are well recognized - it can take the form of delirium, coma, seizures, or late cognitive decline - its pathophysiology is incompletely understood.

Although pathophysiology of SAE has not been established, several likely mechanisms have been proposed. The hallmarks are thought to comprise diffuse neuroinflammation likely driven by initial blood-brain barrier (BBB) leakage leading to microglial activation and altered neurotransmission. Activation of brain microvascular endothelial cells as the primary constituent of the BBB is regarded as an early event, induced by interaction with pathogen product like LPS via pattern recognition receptors and proinflammatory factors.

Microglial cells as the main cell population of resident immune-competent cells in the CNS are activated early after infection-induced systemic inflammation. Cross talk between resident immune cells in the brain, the vascular endothelium and circulating leukocytes probably is responsible for the major part of microglial activation during sepsis. Once activated, microglia exhibit a spectrum of phenotypes and functions to either exacerbate brain injury or to induce repair and regeneration, depending on different molecular signals received by the microglial receptors. Therefore, a wide variety of partly opposing responses have been described for activated microglia and associated with SAE pathophysiology; however, underlying signal transduction pathways are hitherto poorly characterized and appropriate specific treatment options are missing.

Phosphoinositide 3-kinase γ (PI3Kγ) was originally characterized as a signaling protein mediating G protein-coupled receptor stimulation by its enzymatic activity to produce phosphatidylinositol 3,4,5-trisphosphate for downstream protein kinase B/Akt activation. Subsequent studies revealed that PI3Kγ attenuates the cAMP/PKA pathway by working as an activator of phosphodiesterases, which hydrolyze cAMP to 5′-AMP. Recently, we have disclosed PI3Kγ as a key mediator of microglial cell functions at different pathologies including SAE.

Thermoregulation is a fundamental homeostatic function of all mammals that includes three components: afferent thermal sensing, central regulation, and an efferent response. Lower deviation of core body temperature (T_c) outside a small physiological range of circadian variation

lead to rigorous autonomic thermoregulatory responses, mainly driven by a gradually increased sympathetic tone, in order to minimize radiant heat loss by skin vasoconstriction and maximize heat production by brown adipose tissue thermogenesis. Recent data clearly indicate that poor outcome of sepsis is associated with spontaneous T_c lowering (hypothermia, indicating for energy exhaustion) or fever inducing high energy cost as additional physiological challenges in patients with septic life-threatening conditions. Subgroups of patients with increased risk to develop sepsis such as trauma or burns are endangered for cold challenge leading frequently to accidental hypothermia. However, role of challenged thermoregulation upon exposition at reduced ambient temperature (T_a) and possibly resulting accidental hypothermia in pathogenesis of SAE has not been studied.

The aim of this study was to examine the specific role of reduced T_a exposition with probably enhanced sympathetic tone on BBB dysfunction induced by systemic inflammation at the organismic, organ and molecular level.

Experiments were performed in PI3Kγ wild-type, knockout, and kinase-dead mice, which were kept at neutral (30±0.5 °C) or moderately lowered (26±0.5 °C) T_a. Mice were exposed to LPS-induced SIRS and monitored for thermoregulatory response and blood-brain barrier (BBB) integrity. Primary microglial cells and brain tissue derived from treated mice were analysed for inflammatory responses and related cell functions.

We found that a moderate reduction of T_a led to enhanced hypothermia of mice undergoing LPS-induced SIRS accompanied by aggravated SIRS-induced SAE. The data showed an increased BBB disruption under reduced T_a after LPS stimulation, especially in PI3Kγ$^{-/-}$ mice compared to WT and PI3Kγ$^{KD/KD}$ mice. PI3Kγ deficiency enhances BBB injury and upregulation of matrix metalloproteinases (MMPs) as well as an impairment of microglial phagocytic activity.

This study reveals that enhanced adaptive thermoregulatory mechanisms in response to temperatures below the thermoneutral range of T_a and lead to exacerbated LPS-induced BBB injury and accompanied neuroinflammation. The signaling protein PI3Kγ was characterized as a critical mediator of key microglial cell functions involved in LPS-induced BBB injury and accompanied neuroinflammation. PI3Kγ serves a protective role in that it suppresses MMP release, maintains microglial motility and reinforces phagocytosis leading to improved brain tissue integrity.

Zusammenfassung

Sepsis-assoziierte Enzephalopathie (SAE) ist die häufigste Eenzephalopathie-Form, die bei kritisch kranken Patienten auftritt und stellt eine akute neurologische Dysfunktion bei extrakranieller Sepsis dar. SAE ist ein frühes Merkmal einer systemischen Infektion, weist eine hohe Prävalenz bei septischen Patienten schon bei Erstvorstellung (bei bis zu 30%) auf und ist mit erhöhter Mortalität septischer Patienten assoziiert. Obgleich die SAE-Symptome eindeutig festgestellt werden können (Delirium, Koma, Krämpfe oder späte kognitive Einschränkung), ist die Pathophysiologie der SAE immer noch inkomplett aufgeklärt.

Die Pathophysiologie der SEA bislang ist unzureichend aufgeklärt. Jedoch sind eine Reihe wahrscheinlicher Mechanismen inzwischen postuliert worden. Der entscheidende Schädigungsmechanismus besteht offensichtlich in dem Auftreten einer diffuse Neuroinflammation, die wahrscheinlich hervorgerufen wird durch eine initiale Schädigung der Blut-Hirnschranke (BHS). Dies hat eine Mikroglia-Aktivierung und eine veränderte Neurotransmission zur Folge. Eine Aktivierung der zerebralen mikrovaskulären Endothelzellen als primärer BHS- Bestandteil wird dabei als frühes Ereignis angesehen, das durch Interaktion mit pathogenen Substanzen wie z. B LPS via Stimulation von sog. Pattern Recognition Rezeptoren (PRR) bzw. anderen proinflammatorischen Faktoren induziert wird.

Mikroglia-Zellen als die Hauptpopulation residenter immunkompetenter Zellen des ZNS werden schon früh nach Induktion einer infektions-induzierten systemischen Entzündungsreaktion aktiviert. Wechselseitige Interaktionen zwischen den residenten Immunzellen des Gehirns, dem Gefäßendothel und zirkulierende Leukozyten sind augenscheinlich hauptsächlich für die mikrogliale Aktivierung bei Sepsis verantwortlich. Aktivierte Mikrogliazellen zeigen ein Spektrum verschiedener Phänotypen und Funktionen, die entweder zu einer Verschlimmerung der Hirnschädigung beitragen können, oder Reparatur- und Regenerationsprozesse unterstützen. Dies hängt von der Art und Intensität einer großen Vielzahl molekularer Signale ab. Insgesamt wurde bislang eine breite Palette von z.T. gegensätzlichen Reaktionsmustern von aktivierten Mikrogliazellen beschrieben, die als assoziiert mit der SAE-Pathophysiologie gelten. Bislang sind jedoch die zugrunde liegenden Signaltransduktionswege kaum charakterisiert und spezifische Therapieoptionen fehlen gänzlich.

Phosphoinositid 3-kinase γ (PI3Kγ) wurde initial als G-Protein-gekoppeltes Signalprotein charakterisiert, das nach Stimulation mit seiner Enzymaktivität durch Produktion von Phosphatidylinositol 3,4,5-trisphosphat zur Aktivierung der Proteinkinase B/Akt führt. Nachfolgende Untersuchungen wiesen nach, dass PI3Kγ den cAMP/PKA-Signalweg durch Aktivierung

von Phosphodiesterasen, die cAMP zu 5'-AMP hydrolisieren, inhibieren kann. In letzter Zeit wurde von unserer Arbeitsgruppe nachgewiesen, dass PI3Kγ eine Schlüsselstellung bei der Vermittlung mikroglärer Zellfunktionen zukommt, die bei einer Reihe verschiedener Erkrankungen einschließlich der SAE bedeutsam sind.

Die Thermoregulation ist eine fundamentale homöostatische Funktion aller Säugetiere, die drei Komponenten einschließt: Die afferente Temperaturwahrnehmung, die zentrale Regulation und eine efferente Vermittlung der regulatorischen Antwort. Variationen der Körperkerntemperatur (KKT) außerhalb des engen physiologischen Bereiches der zirkadianen Schwankungen führt zu erheblichen autonomen thermoregulatorischen Reaktionen, die hauptsächlich durch graduelle Steigerung des Sypathikotonus vermittelt werden und zu einer Minimierung des Wärmeverlustes durch Vasokonstrikion der Hautgefäße und Maximierung der Wärmeproduktion durch metabolische Thermogenese führen. Aktuelle Daten belegen, dass eine Verschlechterung des Outcomme bei Sepsis mit spontaner Unterschreitung der KKT (Hypothermie, das eine energetische Erschöpfung anzeigt), oder Fieber (mit erhöhtem Energiebedarf) assoziiert ist. Eine Aktivierung der Thermoregulation stellt offensichtlich eine ungünstige zusätzliche Anforderung an Patienten mit lebensbedrohlichen Erkrankungen dar. Patientengruppen mit einem erhöhten Risiko für Sepsis (z. B. Trauma- oder Verbrennungspatienten) sind insbesondere gefährdet, eine Unterkühlung zu erleiden. Dies führt sehr häufig zu akzidenteller Hypothermie. Die pathogenetische Bedeutung von verstärkter Thermoregulation infolge verminderter Umgebungstemperatur und die gegebenenfalls hervorgerufenen Folgen einer akzidentellen Hypothermie für die Pathogenese der SAE wurden bisher nicht untersucht.

Ziel der vorliegenden Untersuchung bestand darin, aufzuklären, ob einer reduzierten Umgebungstemperatur (d.h. Unterschreiten der Neutralzone) mit dadurch induzierter Erhöhung des Sympathikotonus eine eigenständige Bedeutung in der Pathogenese einer BHS-Schädigung infolge systemischer Inflammation zukommt.

Die Experimente wurden an PI3Kγ Wildtype, Knockout (PI3Kγ$^{-/-}$) and Kinase-Dead (PI3Kγ$^{KD/KD}$)-Mäusen durchgeführt, die entweder bei neutraler (30±0.5 °C) oder moderat verminderter (26±0.5 °C) Umgebungstemperatur gehalten wurden. Bei den Mäusen wurde durch LPS-Gabe eine systemische Inflammation (SIRS) induziert. Die thermoregulatorischen Reaktionen wurden fortlaufend telemetrisch und am Versuchsende hinsichtlich der BHS-Integrität erfasst. Außerdem wurden in Zellkultur-Untersuchungen an primären Mikrogliazellen und im Hirngewebe behandelter Mäuse Reaktionsmuster induzierter Neuroinflammation und zugehöriger Zellfunktionen analysiert.

Wir konnten nachweisen, dass eine moderate Verminderung der Umgebungstemperatur zu verstärkter Hypothermie bei LPS-induzierter SIRS und einer Verschlimmerung der SIRS-induzierten SAE führt. Weiterhin konnte gezeigt werden, dass es zu einer verstärkten BHS-Schädigung insbesondere bei PI3Kγ$^{-/-}$-Mäusen im Vergleich mit Wildtyp- und PI3Kγ$^{KD/KD}$-Mäusen kommt. PI3Kγ –Defizit verstärkte die BHS-Schädigung, führte zur verstärkten Upregulation von Matrix-Metalloproteinasen und beeinträchtigte die mikrogliale Phagozytose-Aktivität.

Durch diese Untersuchung konnte nachgewiesen werden, dass eine verstärkte Aktivierung adaptiver Thermoregulationsmechanismen infolge Unterschreitung der Neutralzone der Umgebungstemperatur eine Exazerbation der LPS-induzierten BHS-Schädigung und zugehörigen neuroinflammatorischen Antwort zur Folge hat. Das Signalprotein PI3Kγ konnte als wesentlicher Vermittler von Schlüsselfunktionen der Mikroglia bei LPS-induzierter BHS-Schädigung und zugehörigen neuroinflammatorischen Reaktionen charakterisiert werden.

Aus den vorliegenden Ergebnissen kann die Schlussfolgerung gezogen werden, dass das Signalprotein PI3Kγ als protektiver Faktor wirksam wird, indem die Freisetzung von Matrixmetalloproteinasen supprimiert und die mikrogliale Motilität bzw. Phagozytoseaktivität aufrechterhalten wird.

1. Introduction

1.1. Sepsis - brief historical overview, current definition and incidence

Sepsis is one of the oldest and most elusive syndromes described in medicine. With the confirmation of the germ theory by Semmelweis, Pasteur, and others, sepsis was recast as a systemic infection, often described as "blood poisoning" and assumed to be the result of the host's invasion by pathogenic organisms that then spread by the bloodstream. Before that, Hippocrates firstly claimed that sepsis was the process by which flesh rots, swamps generate foul airs, and wounds fester and Galen later considered sepsis a laudable event, necessary for wound healing (Funk et al. 2009; Majno 1991). However, even with the advent of modern antibiotics consequently to the discovery of pathogenic organism's involvement; germ theory did not fully explain the pathogenesis of sepsis: many patients with sepsis died despite successful eradication of the inciting pathogen. Thus, researchers suggested that it was mainly the host response, not just the germ violence that drove the pathogenesis of sepsis (Cerra 1985). In 1992, an international consensus panel defined sepsis as a systemic inflammatory response syndrome (SIRS) which is frequently caused by infection (Stearns-Kurosawa et al. 2011). Furthermore, septicemia was neither a necessary condition nor a helpful term (Bone et al. 1992). According to the classical definition of sepsis, which was used until two years ago, sepsis diagnosis requires the recognition of the SIRS, which is frequently caused by infection (Stearns-Kurosawa et al. 2011). For a long time, when SIRS occurred with infection, the diagnosis for the patient was sepsis, and the severity of the disease depended on its association with organ dysfunction, hypoperfusion or hypotension. In particular, patients met the criteria for septic shock when they had persistent hypotension and perfusion abnormalities despite adequate fluid resuscitation (Levy et al. 2003). Ongoing advances in molecular biology have provided keen insight into the complexity of pathogen and alarm recognition by the human host and important clues to a host response that has gone awry (Angus and van der Poll 2013). Progress in clinical and translational sepsis research is meanwhile continuously reviewed and consecutively transferred into guidelines in order to improve sepsis diagnosis and therapy (Dellinger et al. 2013).

Meanwhile, the recognition has prevailed that development of organ dysfunction discriminates sepsis from uncomplicated infection. Consequently, the appearance of the new sepsis-3 definition, published two years ago, prompted a reappraisal of organ dysfunction as the hallmark of sepsis. Sepsis is now defined as life-threatening organ dysfunction caused by a dysregulated host response to infection (Singer et al. 2016). Nevertheless, the complex pathogenesis of sepsis remains insufficiently explored and resulting therapeutic concepts are hitherto frequently unable to treat curatively patient suffered from sepsis and septic shock. A complex and dynamic interaction exists between pathogens and host immune-defence mechanisms during

the course of invasive infection. It is now widely thought that the host response to sepsis involves many, concomitant, integrated, and often antagonistic processes that involve both exaggerated inflammation and immune suppression. It has become apparent that infection triggers a complex, variable, and prolonged host response, in which both proinflammatory and anti-inflammatory mechanisms can contribute to clearance of infection and tissue recovery or organ injury and secondary infections (Angus and van der Poll 2013). Several novel mediators resulting from disturbed host tissue and pathways have been shown to play a part. Moreover, evidence is accumulating that microbial virulence and bacterial load contribute to the host response and the outcome of severe infections (van der Poll and Opal 2008). Improved integrative understanding is needed to distinguish the hierarchy of the various mechanisms underlying multi-organ failure as a key consequence of severe sepsis often causative for fatal outcome (Bauer et al. 2018; Rudiger et al. 2008).

Sepsis and septic shock remain major challenges in medicine. Mortality rate is high and its incidence is increasing worldwide (Angus and van der Poll 2013). Recent data from Germany revealed a sustained high number of 88,000 patients with so-called severe sepsis or septic shock in 2011 in German hospitals, with associated hospital mortality rates of 43% for severe sepsis and 60% for septic shock, respectively (Heublein et al. 2013).

The clinical process usually begins with infection, which potentially leads to organ dysfunction following a continuum of severity from sepsis or septic shock leading to multiple organ dysfunction (MOD) and probably death (Gustot 2011). Organ dysfunction or organ failure caused by a dysregulated host response to infection is now defined to be the characteristic clinical sign of sepsis, as mentioned above (Singer et al. 2016); and no organ system is immune from the consequences of the inflammatory excesses induced by an uncontrolled infection. However, the molecular mechanisms that underlie organ failure in sepsis have been only partially elucidated.

Currently, new conceptual thinking is focusing on sepsis as a pathogen-induced imbalance of host damage and repair processes that trigger failure of either resistance or "disease tolerance" mechanisms (Bauer et al. 2018; Medzhitov et al. 2012). These mechanisms provide tissue damage control and repair to sustain host tissue integrity and organ function even without reducing pathogen (Kotas and Medzhitov 2015; Soares et al. 2014).

1.2. Sepsis-associated encephalopathy

Sepsis-associated encephalopathy (SAE) is characterized as diffuse brain dysfunction occurring in response to an organismic infection but accompanies in the absence of direct CNS infection, structural abnormality or other types of encephalopathy (Gofton and Young 2012). Importantly, SAE is a highly relevant clinical problem with a prevalence of up to 30% in septicemic patients at admission. Depending on the study, 30-70% of in-hospital patients with sepsis and SIRS develop SAE (Ebersoldt et al. 2007; Siddiqi et al. 2006). Consequently, the currently recommended score to identify patients with suspected infection who are at risk of sepsis as a life-threatening organ dysfunction due to a dysregulated host response to infection, the quick Sequential [Sepsis-related] Organ Failure Assessment (qSOFA) score, include estimation of altered mentation as one out of three clinical criteria (Seymour et al. 2016).

Intriguingly, a relevant part of sepsis survivors suffers from long-term cognitive deficits, (impaired attention and memory as well as verbal fluency difficulties). Therefore, sepsis is a great risk for developing new permanent neurocognitive dysfunction especially in the elderly affecting their ability to live independently (Semmler et al. 2013; Widmann and Heneka 2014).

Till now no specific biomarker exists for SAE and it remains therefore a clinical diagnosis (Gofton and Young 2012). SAE manifests as a spectrum of disturbed cerebral function ranging from mild delirium to coma. As mortality is increased with severity of SAE (Zhang et al. 2012), early identification and management of patients with SAE are important to reduce associated morbidity and mortality. Patients presenting with SAE show evidence of severe systemic infection with features of sepsis or SIRS (Young et al. 1990). Cerebral dysfunction seen in SAE reflects the systemic metabolic, inflammatory and haemodynamic disturbances that are associated with SIRS, rather than a direct CNS abnormality (Fig. 1). Nevertheless, detailed pathophysiology of SAE has not been completely understood (Gofton and Young 2012; Tauber et al. 2017).

In general, SAE pathophysiology involves BBB dysfunction and neuroinflammation caused by endothelial and microglial activation induced by endogenous or pathogen-derived compounds. Furthermore, hypoxia by impaired microvascular regulation and septic shock as well as imbalance of neurotransmitters contributes to SAE severity (Mazeraud et al. 2016).
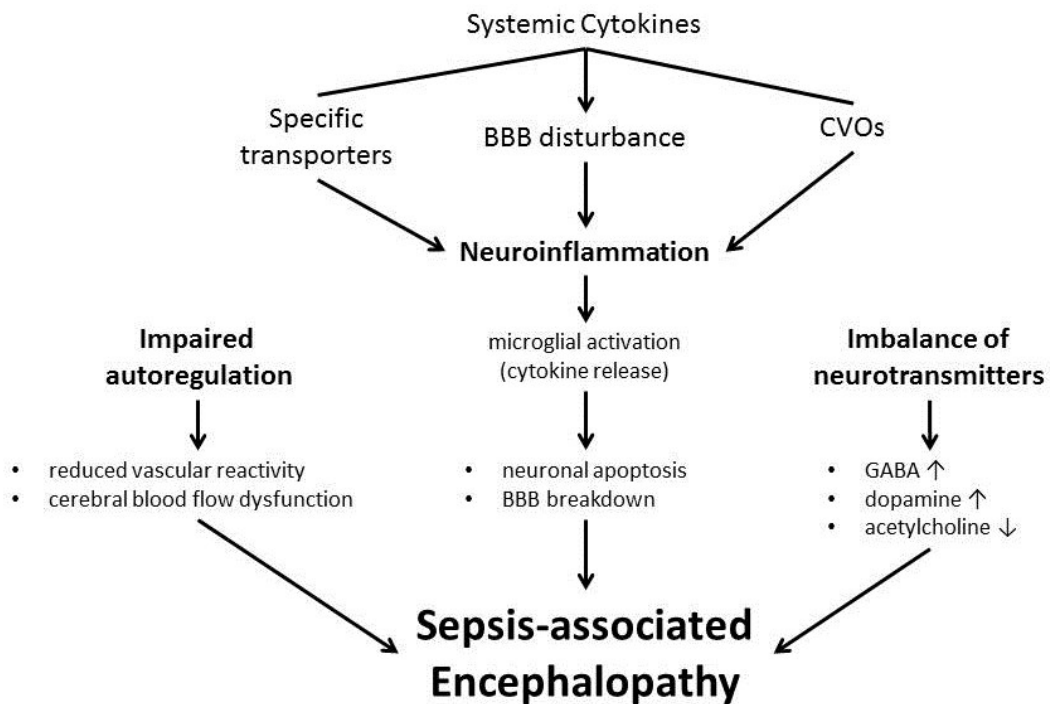
Figure 1. Pathophysiology of sepsis-associated encephalopathy.
Three mechanisms contribute to SAE: (I) Systemic cytokines enter the CNS either by specific transporter uptake or via the disturbed BBB or directly via the circumventricular organs (CVOs), induce the activation of microglial cells, which leads to further BBB breakdown and neuronal apoptosis, (II) impaired autoregulation lead to reduced vascular reactivity and cerebral blood flow dysfunction, (III) imbalance of neurotransmitters. GABA: gamma-aminobutyric acid. Adopted from (Tauber et al. 2017).

1.2.1. BBB disturbance and neuroinflammation at SAE onset - Role of PI3Kγ

Infection-induced response of systemic inflammation is thought to be mainly responsible for SAE initiation due to BBB breakdown. This pathological process is triggered by an early and overwhelming release of proinflammatory cytokines from innate immune cells triggered by microbial particles (PAMPs - pathogen-associated molecular patterns) and recognized by toll-like receptors (TLRs) and other pattern recognition receptors (PRRs) (Ebersoldt et al. 2007; Laflamme and Rivest 2001). The hallmark of early SAE propagation is thought to be a diffuse neuroinflammation driven by microglial activation due to BBB leakage leading to direct cellular neuronal damage. Subsequently, significant deterioration of brain endothelial tight junctions allows invasion of blood-born immunocompetent cells and corresponding proinflammatory reinforcement (Nag et al. 2011). Because our experimental study presented herein is focused on the early manifestation period of SAE, we will restrict the detailed description of the known SAE pathogenesis on this period of disease.

Till now, it is partly understood how a systemic inflammation affects the brain and leads to SAE, considering that the healthy brain is well protected to the outside by the BBB. The barrier

functions of the capillary bed of the brain are known to arise from three modifications: the presence of tight junctions between endothelial cells (ECs), a near absence of macropinocytosis, and loss of fenestrae (Brightman and Reese 1969; O'Brown et al. 2018; Reese and Karnovsky 1967).

It has been shown that the fraction of circulating bacterial product entering the brain via unaffected BBB appears to be low (Banks and Robinson 2010). Nevertheless, these mouse studies showed that LPS uptake into the brain (dosages comparable with usually used doses to induce SIRS by intraperitoneal application) is high enough to activate brain parenchymal TLR4 receptors. Therefore, microglial cells at the surveillance state appears to be prone to become activated during the initial period of SIRS by direct interaction with low dose PAMPs originated from extracerebral sources.

However, interaction between microbial particles (acting as PAMPs) with the luminal surface of cerebral endothelial cells - as an integral BBB component - contribute to the mediation of neuroinflammatory response considerably because about 75%, of the circulating LPS that does interact with the BBB is reversibly binding to the luminal surface of the BBB leading to activate the ECs (Banks and Robinson 2010). In consequence, a considerable vasodilation and serum protein extravasation appeared already 4 hours after LPS application indicating BBB breakdown, caused by NO synthase (NOS) activation (Mayhan 1998). Furthermore, cerebral ECs express Toll-like receptors (TLRs) which are themselves by oxidative stress and TNFα (Nagyoszi et al. 2010) and are activated to release proinflammatory cytokines, including TNFα and IL-1β in both luminal and abluminal directions (Erickson and Banks 2018; Nagyoszi et al. 2015). Intriguingly, cerebral ECs secrete various cytokines in a polarized manner, i.e., response to neuroimmune stimulation by LPS occurred more robustly when applied abluminal than did luminal LPS administration (Verma et al. 2006). Therefore, activated ECs contribute directly to initial promotion of neuroinflammation in virtue of peripheral infection.

Another relevant pathways responsible for early propagation of SIRS-induced neuroinflammation are considered to be a transcytic vesicular transport of blood-born macromolecules (i.e., PAMPs or cytokines) though the BBB (Esen et al. 2012; Lossinsky and Shivers 2004) and cytokine transport across the BBB in the blood-to-brain direction by way of saturable transport systems (Banks and Erickson 2010). The latter involve facilitated diffusion and receptor-mediated transcytosis as well as energy-requiring, non-vesicular or pore-dependent transport. The transport systems for major proinflammatory cytokines are constitutively expressed, selective and receptor-mediated as well as cytokines use different routes to enter brain tissue (Banks 2005): Therefore, these immune response modulating cytokines like IL-1β and TNFα, which

are not normally circulating in blood, are immediately transported across BBB to transfer the information of a peripheral innate immune response to an establishing infection into the brain. The resulting neuroinflammatory response appears to be complex and involves behavioral alterations (called sickness behaviors (Dantzer et al. 2008)) and activation of immune competent cells within the neurovascular unit (NVU).

Microglia are resident macrophages of the CNS, represent an integral NVU component and constitute about 5-20% of all cells in the CNS (Kettenmann et al. 2011; Lawson et al. 1990). A hallmark of microglia is their rapid activation after a CNS insult, resulting in their migration toward injury, proliferation, and their change in morphology. They take on a more "amoeboid" shape with shorter and thicker processes and display increased immunoreactivity for Iba-1 (Greter et al. 2015).

Previous work in our lab revealed that PI3Kγ, a signaling protein constitutively expressed in immune competent cells (Wetzker and Rommel 2004), play a crucial role in controlling inflammatory response in microglial cells. Few years ago, we and others showed that PI3Kγ is expressed in microglial cells and is upregulated under proinflammatory conditions (Jin et al. 2010; Schmidt et al. 2013). Ongoing own work revealed that mainly the lipid kinase independent function of PI3Kγ (detailed explanation, see below) was responsible for the immune modulating activity of PI3Kγ. Indeed, it could be shown that - with exception of its migration-stimulating effect (Schneble et al. 2017b) - control of cAMP signaling was responsible for suppressive effects of proinflammatory cell functions in activated microglial cells in cell culture as well as in mouse models of several serious diseases. Our group characterized the PI3Kγ - mediated stimulation of cAMP phosphodiesterase activity as a crucial factor of microglial phagocytosis (Schmidt et al. 2013). Subsequent studies on SIRS-induced neuroinflammation revealed the lipid kinase independent function of PI3Kγ as a crucial mediator of microglial cell activation, MMP expression and activation with subsequent BBB deterioration (Frister et al. 2014). Parallel investigations on *in vivo* and *in vitro* models of brain ischemia have shown that PI3Kγ is essential for microglial cAMP regulation under such pathological conditions and its loss provoked an increased MMP-9 expression and suppressed phagocytic activity leading to enhanced brain damage after focal brain ischemia (Schmidt et al. 2016).

Therefore, suppressive effect of PI3Kγ on cAMP levels appears critical for the restriction of overwhelming neuroinflammatory activity of microglial cells and its consequences for enhanced brain injury.

1.3. Role of ambient temperature for homeothermy in mice and men

Thermoregulation is a fundamental homeostatic function of all mammals that is governed by the CNS in homeothermic animals. In humans, body temperature is therefore tightly controlled within a narrow range of 0.2-0.4 °C by coordinated hypothalamic functions. The central thermoregulatory system also functions for host defense from invading pathogens by elevating body core temperature, a response known as fever. In order to warrant homeothermism, three components are established: afferent thermal sensing, central regulation, and an efferent response (Nakamura 2011). Thermoregulation involves therefore a variety of involuntary effector responses, such as non-shivering thermogenesis in brown adipose tissue, shivering thermogenesis in skeletal muscles, thermoregulatory cardiac regulation, heat-loss regulation through cutaneous vasomotion, sweating, piloerection and metabolic regulation via endocrine control regulated by adrenocorticotropic hormone (ACTH) release. To defend thermal homeostasis from environmental thermal challenges, feedforward thermosensory information on environmental temperature sensed by skin thermoreceptors ascends through the spinal cord to the preoptic area (POA) of the hypothalamus. Variations in T_c outside this range lead to autonomic thermoregulatory responses, mainly driven by a gradual modulation of the sympathetic tone (Charkoudian and Wallin 2014).

Homoeothermic living organisms spend a certain part of energy to maintain T_c. However, the percentage varies considerably and depends basically from body surface area to mass ratio and whole body thermal conductance. Therefore, mice compared to (naked) human beings have to invest about 10 times more energy for this purpose (Gordon 2012). Intriguingly, both species share a similar rage of ambient temperature (T_a, 28-32 °C), where the energy expenditure is minimal (thermoneutral zone, TNZ). Mouse have a ~7-fold higher mass-specific metabolic rate than human beings (Schreiber et al. 2017; West et al. 1997). Nevertheless, mice are just able to stabilize T_c under thermoneutral T_a by help of periodic motor activity. Indeed, during sleep T_c goes down by 1-2 °C within around 1h which then induces arousal and a short period of exercise provokes an appropriate T_c upgrade ((Jhaveri et al. 2007), own unpublished observations).

Underrun as well overrun of TNZ result in immediate and increasing energy expenditure, which may influence time course and severity of potentially life-threatening diseases such as sepsis (Schortgen 2012). Interestingly, there are different strategies to respond on T_a challenges in mice and human beings. Heat stress can be effectively handled by men with sweating which allows living and working at T_a higher than T_c. However, mice develop hyperthermia already

when T_a transcended TNZ by 2 °C (Gordon 2009) and further increase in T_a will enhance danger for life-threatening heatstroke (Leon et al. 2010).

In contrast, a shortfall of the lower critical temperature (LCT) of TNZ, that means the threshold for activation of a regulatory response by the thermoregulatory system where additional heat must be generated to meet the demand for increased heat loss (~29 °C), discloses mice to be considerably more effective and use additional mechanisms to save energy as it is possible for human beings. Mice are able to stabilize T_c in a T_a range of 18-28 °C, but just mildly reduced at T_a of 12 °C and 4 °C (Abreu-Vieira et al. 2015). There is a continuous increase of food intake and energy expenditure of ~50% more when T_a was reduced to 22 °C and ~120% at a T_a of 4 °C (Abreu-Vieira et al. 2015; Gordon et al. 2017). In human beings homeothermy is quite tightly regulated. Therefore, a maximal heat production is initiated with ~5fold increase of O_2 consumption - mainly by shivering - already at a beginning hypothermia (T_c reduction of ~1 °C) (Eyolfson et al. 2001; Sessler 2016). Therefore, accidental (mild) hypothermia due to undercooling or in consequence from disturbed thermoregulation is prone to worsen time course and severity of serious diseases like trauma, burns or sepsis mainly because of enhanced energy exhaustion (Cumming et al. 2001; Schortgen 2012; Soreide 2014).

A serious difference in thermoregulatory performance between mice and men consists in different response on mild to moderate hypothermia, e.g. the reduction of T_c between 35 and 28 °C. Whereas human beings develop serious cardiovascular, renal, cerebral and respiratory disturbances including coagulopathies, immune suppression and life-threatening cardiac arrhythmias (Brown et al. 2012; Danzl and Pozos 1994), healthy mice are able to cope with hypothermia < 25 °C due to starvation or hypoxia as a principle of energy saving (torpor) (Jensen et al. 2013; Overton and Williams 2004; Swoap 2008).

Despite their more efficient ability to cope with cold stress, mice are valuable animal models for preclinical studies in order to evaluate the impact of environmental conditions, especially T_a on time course and pathophysiology of serious diseases like systemic inflammation and sepsis. They fulfill with their feature to develop no serious complications like arrhythmias or bleedings due to hypothermia a cardinal prerequisite of a model: simplification. Furthermore, they allow a causal interpretation of potential different phenotypes by usage of targeted mutants.

1.4. Phosphatidylinositol 3-kinases

1.4.1. The PI3K family

Phosphatidylinositol 3-kinases (PI3Ks) are members of a unique and conserved family of enzymes responsible for the phosphorylation of proteins and lipids. Few information are available about the protein kinase function of PI3Ks (Thomas et al. 2013), while the lipid kinase activity of these enzymes has been extensively studied (Vanhaesebroeck et al. 2010). PI3Ks function is to phosphorylate phosphatidyl-inositol lipids at the D3 position of the inositol ring (Cantley 2002). PI3Ks are usually activated in response to cell stimulation by growth factors and hormones, and they contribute to many intracellular processes including cell survival, cell proliferation, metabolism, cell growth, migration and intracellular trafficking (Engelman et al. 2006; Hirsch et al. 2007). PI3K-produced 3-phosphoinositides regulate intracellular processes through the recruitment of signaling proteins at the plasma membrane, whereby they become activated (Cantley 2002).

According to their lipid substrate preferences and to their structural features, PI3Ks are divided into three classes (Class I, Class II and Class III) based on their structural and biochemical features (Leevers et al. 1999; Vanhaesebroeck et al. 2010).

Vps34, was found to encode a PI3-kinase that specifically PtdIns at the D-3 position of the inositol ring to produce PtdIns3P is the only known member of class III PI3K and it is also the only PI3K expressed in all eukaryotic cells (Leevers et al. 1999). Class II PI3Ks includes three catalytic isoforms (C2α, C2β, and C2γ), but their functions are less well understood. Class II PI3K catalyzes the production of PIP from PI and the production of phosphatidylinositol (3,4)-bisphosphate (PIP_2) from phosphatidylinositol 3-phosphate (PIP). Although recent studies have pointed to a role of class II and III PI3Ks in vesicular trafficking (Franco et al. 2014) and cell growth (Odorizzi et al. 2000), class I PI3Ks still represent the best characterized subfamily. Class I PI3Ks, *in vivo*, primarily convert phosphatidylinositol-4,5-bisphosphate (PIP_2) into phosphatidylinositol-3,4,5-trisphosphate (PIP_3), which interacts with numerous signaling proteins with pleckstrin-homology (PH) domains. Thus, PIP_3 is known to bring the protein serine-threonine kinases Akt (alternatively called protein kinase B, PKB) and phosphoinositide-dependent kinase 1 (PDK1) into proximity, facilitating Akt phosphorylation (Alessi et al. 1996). Activated Akt phosphorylates and regulates compound proteins, such as glycogen synthase kinase 3 beta (GSKβ), forkhead-box-protein O (FOXO) and others, thus triggering multiple intracellular signaling cascades (Cantley 2002; Engelman et al. 2006). All these PI3K-induced signaling pathways are controlled and limited by protein phosphatases, which degrade PIP_3. Of

note, Src homology 2 (SH2)-containing-phosphatases (SHIP1 and SHIP2) and phosphatase and tensin homolog (PTEN) dephosphorylate PIP$_3$ in positions D5 and D3 respectively, thus terminating PI3K signaling (Cantley 2002; Laurent et al. 2014).

All class I PI3Ks are heterodimers of a p110 catalytic subunit and a regulatory subunit. Depending on the activation mechanism and the differential association with regulatory subunits, class I PI3Ks have been grouped in two subfamilies, class IA and class IB (Engelman et al. 2006; Vanhaesebroeck et al. 2010; Vanhaesebroeck et al. 1997). Class IA catalytic subunits (p110α, p110β and p110δ) bind to the p85 type of regulatory subunits, containing SH2 domains which are able to bind phosphorylated tyrosine on receptor tyrosine kinases (RTKs) (Burke and Williams 2013). On the contrary, class IB catalytic subunit (p110γ) binds two other regulatory subunits, p101 and p84/87, which facilitate the direct binding with G$_{βγ}$ subunit of trimeric G proteins (Stephens et al. 1997) (Fig. 2).
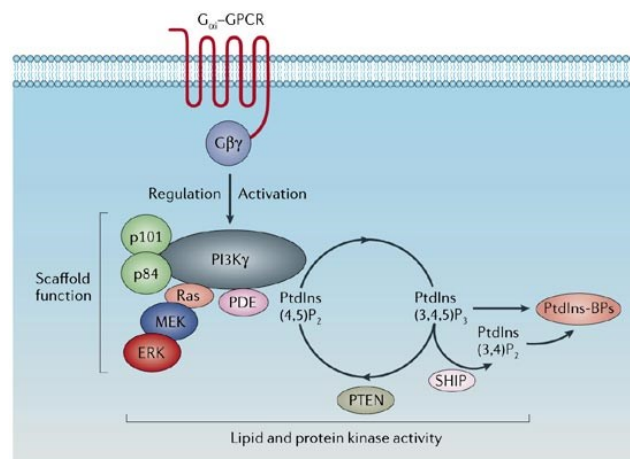
Figure 2. Brief overview of PI3Kγ structure and function

Detailed description is referred in the text; GPCR, G protein coupled-receptor; PDE, Phosphodiesterase; MEK, mitogen-activated protein kinase (MAP) kinase; ERK, extracellular-signal-regulated kinase; PTEN, phosphatase and tensin homolog; SHIP, SH2-containing inositol 5-phosphatase, adopted from (Ruckle et al. 2006).

1.4.2. PI3Kγ: Kinase-dependent and -independent functions

As mentioned above, PI3Kγ is the only member of class IB family (Stoyanov et al. 1995). Its lipid kinase activity generates PIP$_3$ to recruit and activate downstream signaling molecules in order to mediate a wide variety of biological processes, such as inflammation, cardiac remodeling, dendritic cell migration, thrombus formation and allergic responses (Costa et al. 2011; Hirsch et al. 2000; Nienaber et al. 2003; Wymann and Solinas 2013). It can be activated by G protein coupled receptors (GPCR) (Hirsch et al. 2000) or also by pro-inflammatory cyto-

kines (Johnson et al. 2004). PI3Kγ activation is mediated by the interaction of its catalytic domain with the βγ-subunits of G proteins or Ras. Some proteins including Ras, mitogen-activated protein kinase (MAPK), phosphodiesterases (PDE), p101 and p84, are able to bind to PI3Kγ, indicating a protein-scaffold function activating other signaling molecules by protein-protein interaction (Hirsch et al. 2009). Remarkably, PI3Kγ enzyme can form a multiprotein complex containing cAMP-degrading phosphodiesterases, thus negatively regulating cAMP pools (Patrucco et al. 2004; Schmidt et al. 2013). Specifically, it has been shown in cardiomyocytes that PI3Kγ directly interacts with the phosphodiesterase 3B (PDE3B) isoform, thus controlling cAMP-induced heart contractility (Patrucco et al. 2004). Furthermore, could be shown that the suppressive effect of PI3Kγ on the intracellular cAMP level of microglial cells appears critical for the restriction of overwhelming immune functions in virtue of different acute brain injuries (Frister et al. 2014; Schmidt et al. 2016).

Altogether, these studies underlined that there is a connection between PI3Kγ kinase-dependent and -independent functions, previously described as distinct signaling pathways. However, the interaction partners identified to date provide only a hint of a potentially larger set of associations and their functional relevance. New studies will be essential to help uncover additional binding partners of PI3Kγ in health and disease.

1.4.3. Role of PI3Kγ in microglial function

As the immune-competent cells of the brain, microglia play an increasingly important role in maintaining normal brain function. They invade the brain early in development, transform into a highly ramified phenotype, and constantly screen their environment (Nimmerjahn et al. 2005). Microglia are activated by any type of pathologic event or change in brain homeostasis. This activation process is highly diverse and depends on the context and type of the stressor or pathology (Kettenmann et al. 2011; Wolf et al. 2017).

Based on previous studies of our group and others, PI3Kγ is constitutively expressed in microglial cells, which suggest that PI3Kγ is an important mediator in microglia functions. Microglial cells represent the first line of brain cells which respond on any disturbances of cerebral homeostasis. They are morphologically dynamic cells whose morphological changes occur by pathological events in the CNS. Activated microglial cells are capable of migration, phagocytosis, proliferation, reactive oxygen species (ROS) production and the production of various cytokines (Hanisch and Kettenmann 2007). In our previous studies, wild-type (WT), PI3Kγ

knockout (PI3Kγ$^{-/-}$) (Hirsch et al. 2000) and PI3Kγ kinase-dead (PI3Kγ$^{KD/KD}$) mice (Patrucco et al. 2004) were used to clarify the lipid kinase dependent and/or independent function of PI3Kγ. Previous investigations have shown that PI3Kγ act as a vital mediator in microglial ROS formation, MMPs production, phagocytosis and migration (Frister et al. 2014; Schmidt et al. 2013; Schneble et al. 2017b). It has been shown that PI3Kγ aggravates the microglial migration through the lipid kinase-dependent pathway (Schneble et al. 2017b). Furthermore, our findings revealed that the loss of PI3Kγ can enhance BBB disturbance and subsequently increase MMPs expression via lipid kinase-independent control of cAMP in microglial cells (Frister et al. 2014). Results in PI3Kγ$^{-/-}$ mice and PI3Kγ$^{KD/KD}$ mice also indicate PI3Kγ-dependent suppression of cAMP signaling as a critical regulatory element of microglial phagocytosis (Schmidt et al. 2013). Altogether, these findings imply that the suppressive effect of PI3Kγ on cAMP-mediated signaling is mainly responsible for an alleviation of some key features of neuroinflammatory activity in activated microglial cells (Gyoneva and Traynelis 2013), while keeping in mind the anti-inflammatory effect on "resting" microglia induced by β-adrenergic stimulation (Feinstein et al. 2002; Gyoneva and Traynelis 2013).

1.5. Objectives and aim of this study

SAE is a diffuse brain dysfunction which is associated with severe sepsis and has a negative influence on survival. The CNS is one of the first organs affected during sepsis, the primary symptom is a disturbed level of consciousness (Gofton and Young 2012; Molnar et al. 2018). The pathogenesis of SAE includes BBB dysfunction, excessive microglial activation, local generation of pro-and anti-inflammatory cytokines and further proinflammatory events (Papadopoulos et al. 2000; Sonneville et al. 2013). Recent data clearly indicate that poor outcome of sepsis is associated with spontaneous T_c lowering (hypothermia, indicating for energy exhaustion) or fever inducing high energy cost as additional physiological challenges in patients with septic life-threatening conditions (Clemmer et al. 1992; Schortgen 2012; Young et al. 2012). Subgroups of patients with increased risk to develop sepsis such as trauma or burns are endangered for cold challenge leading frequently to accidental hypothermia (Cumming et al. 2001; Soreide 2014). However, role of challenged thermoregulation upon exposition at reduced T_a and possibly resulting accidental hypothermia in pathogenesis of SAE has not been studied.

The aim of this study was to examine the specific role of reduced T_a exposition with probably enhanced sympathetic tone on BBB dysfunction induced by systemic inflammation at the organismic, organ and molecular level.

In order to examine different traits of PI3Kγ signaling on microglial activation, migration and phagocytic activity, PI3Kγ-deficient mice and mice carrying a targeted mutation in the PI3Kγ gene causing loss of lipid kinase activity habituated to neutral or reduced T_a exposition were used to induce SIRS by intraperitoneal endotoxin/LPS administration. Mechanistic considerations were intended to characterize involved signaling pathways using brain tissue assays and immunohistochemical techniques as well as primary cell cultures and were performed to probe putative pathways that could reconcile the physiological and molecular mechanisms of cold adaptation and SAE.

We hypothesize that reduced T_a led to enhanced hypothermia early after LPS induced systemic inflammation.

Enhanced thermoregulatory response in virtue of reduced T_a may increase elevated sympathetic stimulation during the early period of SIRS.

Previous own studies showed that adrenergic signaling was a key mediator for aggravated BBB disturbance owing to LPS-induced SIRS (Frister et al. 2014). Therefore, we assume that a postulated enhancement of the sympathetic activity should provoke a further exacerbation of BBB breakdown in mice kept under reduced T_a.

Microglial cells as resident immune-competent cells of brain parenchyma are known to play a significant pathogenetic role during the early period of SAE manifestation (Frister et al. 2014) and exhibit a constitutive expression as well as an established signaling and control of cell functions of PI3Kγ (Frister et al. 2014; Schmidt et al. 2013; Schneble et al. 2017b). Therefore, we will focus our mechanistic studies on this cell population

In addition, it should be clarified if PI3Kγ lipid-kinase dependent and/or independent mechanisms are able to mediate suppression of microglial inflammatory response induced by LPS-induced SIRS.

For that purpose, a well-characterized mouse model of infection-induced SIRS by intraperitoneal endotoxin/LPS injection was used, which is suited for mechanistic studies with time-critical requirements (Buras et al. 2005). PI3Kγ wild-type, knockout, and kinase-dead mice were exposed to LPS-induced SIRS and assessed for sickness symptoms (Gonnert et al. 2011; Ndongson-Dongmo et al. 2015), T_c dynamics, BBB integrity, and microglial cell functions (migration, phagocytosis). Additionally, primary microglial cells derived from the respective mouse genotypes were used for mechanistic analysis of PI3Kγ effects on microglial inflammatory response.

2. Materials and Methods

2.1. Materials

2.1.1. Chemicals

The chemicals used for experiments of this study were listed in Table 1. A Millipore Synergy UV system (Millipore, USA) was used for the preparation of all the buffers. Unless otherwise stated, all buffers were diluted in double deionized water.

Phosphate-buffered saline solution (PBS: 137mM NaCl, 2.7mM KCl, 1.8mM KH_2PO_4, 10mM Na_2HPO_4, pH7.5) was used as the basis for various solutions, as washing buffer in various applications and for cell culture. The composition of all other buffers and solutions was described in the respective protocols.

Table 1. List of chemicals

Chemicals	Purpose of use	Company
DMEM	Cell culture	Sigma (USA)
Fetal bovine serum	Cell culture	Biowest (FRA)
Pen/strep	Cell culture	Sigma (USA)
Amphotericin B	Cell culture	Sigma (USA)
Trypsin	Cell culture	Thermo Fisher Scientific (USA)
EDTA	Cell culture	Sigma (USA)
Dnase	Cell culture	Thermo Fisher Scientific (USA)
HEPES	Cell culture	Roth (GER)
NaCl	Cell culture/IHC	Roth (GER)
KCl	Cell culture/IHC	Sigma (USA)
KH_2PO_4	Cell culture/IHC	Roth (GER)

Na$_2$HPO$_4$	Cell culture/IHC	Roth (GER)
Poly-L-Lysine	IHC	Sigma (USA)
Tween 20	IHC	Serva (GER)
PFA	IHC	Fischar (GER)
Paraffin	IHC	Merck (GER)
Tri-sodium citrate (dihydrate)	IHC	Fluka (GER)
Xylene	IHC	Roth (GER)
NDS	IHC	Sigma (USA)
BSA-c	IHC	Sigma (USA)
Fluoromount	IHC	Southern Biotech (USA)
Isoflurane	Mouse	CP-Pharma (THA)
Evan´s Blue	Mouse	Sigma (USA)
Zymosan	Phagocytosis assay	Thermo Fisher Scientific (USA)
Crystal Violet	Migration assay	Sigma (USA)

2.1.2. Substances for Stimulation and Antibodies

The substances for stimulation and antibodies used for mouse experiments and histology/immunohistochemistry are listed in Table 2 and Table 3.

Table 2. List of substances for stimulation

Stimuli	Target	Dilution	Company
LPS	Mice	10mg/kg body weight	Sigma (USA)
LPS	Cells	100ng/ml	Sigma (USA)
C5a	Cells	10ng/ml	Sigma (USA)

Table 3. List of antibodies

Target molecule	Purpose of use	Source	Dilution	Species / type
MMP-9	IHC	Cell Signaling (USA)	1:150	Rabbit polyclonal
PMN	IHC	ACCURATE CHEMI-CAL & SCIENTIFIC CO (USA)	1:250	Rabbit polyclonal
Iba1	IHC	Abcam (UK)	1:250	Goat polyclonal
CD31	IHC	Dianova (GER)	1:20	Rabbit polyclonal
Streptavidin Cy3	IHC	Southern Biotech (USA)	1:400	
DAPI	IHC	Sigma (USA)	1:2500/1:1000	
Alexa Fluor®488 donkey anti-rabbit	IHC	Thermo Fisher Scientific (USA)	1:250	Donkey
donkey anti-rabbit IgG biotin	IHC	Jackson Immuno Research (USA)	1:400	Donkey
Alexa Fluor®568 donkey anti-goat IgG antibody	IHC	Thermo Fisher Scientific (USA)	1:250	Donkey

2.2. Methods

2.2.1. Animals and experimental procedures

PI3Kγ knockout mice (PI3Kγ$^{-/-}$) (Hirsch et al. 2000)and mice carrying a targeted mutation in the PI3Kγ gene causing loss of lipid kinase activity (PI3Kγ$^{KD/KD}$) (Patrucco et al. 2004)were on the C57BL/6J background for > 10 generations. Age-matched C57BL/6 mice were used as

controls. The animals were maintained at 12 h light and dark cycles with free access to food and water. The animal procedures were performed according to the guidelines from Directive 2010/63/EU of the European Parliament on the protection of animals used for scientific purposes. Experiments were approved by the committee of the Thuringian State Government on Animal Research.

Animals were divided into a cohort kept at neutral ambient temperature (29.5±0.5 °C) (Gordon et al. 1998) or another cohort kept at lowered ambient temperature (25.5±0.5 °C) during the whole experimental period. After acclimatization for > 5 days mice received LPS (10 mg/kg, intraperitoneal, from Escherichia coli serotype 055: B5, Sigma–Aldrich, St. Louis, USA, Lot #032M4082V) as a single intraperitoneal injection. Additionally, 500 µl saline was injected subcutaneously immediately after LPS administration as well as after 24 h to ensure appropriate fluid resuscitation. Clinical status was estimated at baseline state and 24 h after LPS administration according to (Gonnert et al. 2011), which was based on the behavior and appearance of the mice. The classification of CSS grade was shown in Table 4.

Table 4. Classification of CSS Grade (Gonnert et al. 2011)

CSS level	Quality	Posture	spontaneous activity	Response to stimuli
1	No signs of illness	Normal	High activity	quick, curious
2	Low-grade	Slightly hunched	Less active, interruption of activity	Delayed, but adequate reaction
3	Mid-grade	Hunched	Slow, sleepy, movements restricted	Restricted and delayed reaction
4	High-grade	Severely hunched	lethargic, no movement	No reaction

As an *in vitro* correlate of hypothermia and neuroinflammation, primary microglia obtained from wild type, PI3Kγ$^{-/-}$ and PI3Kγ$^{KD/KD}$ were exposed to an incubation temperature (T$_{Inc}$) of 33 °C and LPS (100 ng/ml).

2.2.2. Telemetric assessment of body core temperature (T$_c$) and heart rate

T$_c$ and heart rate (HR) were assessed by telemetric monitoring of electrocardiography (ECG) and abdominal temperature.

Surgical procedure:

Mice were anesthetized with 2.5% isoflurane in oxygen. A midline incision was made on the abdomen and the intraperitoneal cavity was gently opened. An implantable 1.6-g wireless radiofrequency transmitter (ETA-F10, Data Sciences International, St. Paul, MN) was inserted; the leads were transferred though the abdominal wall and the incision was closed by a surgical suture. The cathodal lead was looped forward subcutaneously to an area overlying the scapula and anchored in place with a permanent suture. The anodal lead was brought subcutaneously to rest near the heart apex. Thereafter skin incision was sutured. A warming light was used to maintain body temperature between 36 and 37 °C. Meloxicam was given for pain on the day of surgery and the following day. Experiments were initiated 10 days after recovery from surgical instrumentation. Animals were monitored continuously by telemetry by ECG as well as body temperature and motor activity recording.

Data acquisition and processing:

For simultaneous ECG and body temperature, analog signals were digitalized by the telemetric receiver (model RPC-1, Data Sciences International, St. Paul, MN) and transferred via DSI Data Exchange Matrix at a sampling rate of 2 kHz with 12-bit precision (acquisition software: Ponemah Software 5.20) without a signal filter and stored on PC for off-line data analysis. Instantaneous heart rate was derived from the reciprocal RR interval time series. Therefore, the individual R-waves, with the R-wave peak as the trigger point, were sequentially recognized (ATISApro®, GJB Datentechnik GmbH, Langewiesen, Germany). Accurate R-wave peak detection was verified by visual inspection. Temperature was continuously measured by the implanted transmitter and stored in parallel to the ECG signal.

2.2.3. Measurement of blood-brain barrier permeability

BBB disruption was analyzed by measurement of Evans blue (EB) extravasation into brain tissue as described previously (Comim et al. 2011; Frister et al. 2014). In brief, EB (4 ml/kg of a 2% solution in PBS) was injected through the tail vein 1 h prior killing. Deeply anaesthetized animals were transcardially perfused with ice-cold PBS (40 ml) 24 h after LPS administration. The brains were removed after blood removal, snap-frozen in liquid nitrogen and stored at -80 °C. One hemisphere was homogenized in trichloroacetic acid (50%) and centrifuged (10,000 rpm, 20 min, 4 °C). Supernatant was diluted in three volumes of ethanol. EB was quantified by fluorescence measurement (Tecan Infinite F200, excitation 620 nm, emission 670 nm) and

compared to a standard curve. EB concentrations are presented as µg of EB per µl of brain tissue supernatant.

2.2.4. Blood and brain tissue cytokine assessment

The cytokines levels (TNFα, IL-6, MCP-1) in blood and brain tissue were determined using BD™ CBA Mouse Inflammation Kit (Dickinson and Company, San Jose, USA). Briefly, the brain tissue was harvested after rinsing with cold PBS, immediately put in liquid nitrogen and kept at -80 °C until processing. The brain tissue was then powdered, ice-cold diluted in PBS, homogenated, centrifuged at 1000 g for 10 min at 4 °C. Supernatant was immediately kept at -80 °C until the measurement.

Cytokines levels (TNFα, IL-6, MCP-1) in blood were also determined using BD™ CBA Mouse Inflammation Kit (Dickinson and Company, San Jose, USA). Briefly, the blood was collected in the heparinized needle via a direct puncture in the heart and immediately centrifuged at 1500 g for 10 min at 4 °C. Supernatant was immediately kept at -80 °C until the measurement.

2.2.5. Preparation of primary microglia

The cell culture medium DMEM with thermally inactivated fetal calf serum (FCS, 10% v/v), Penicillin (100 units/ml), Streptomycin (100 µg/ml) and Amphotericin B (2,5 µg/ml) was used as the primary microglia culture medium. Primary microglial cells were isolated from the cerebral cortex of newborn C57BL/6J wild-type (WT), PI3Kγ-knockout (PI3Kγ$^{-/-}$) and PI3Kγ kinase-dead (PI3Kγ$^{KD/KD}$) mice (1-3 days after birth). The brains were collected and washed with PBS. The cortex hemispheres were separated after removing the meninges thoroughly, dissociated with dissociation solution (20 mM Hepes, 0.05% m/v Trypsin, 700 µM EDTA, 12 µg/ml DNase in DMEM) and incubated for 20-30 min at 37 °C with gently mixing from time to time. After incubation, the cortex hemispheres were transferred to microglia culture medium (10% FCS, 1% penicillin, 1% amphotericin B) and triturated with a Pasteur-pipette. Then the cells were seeded into a T75 flask. The cells were co-cultivated with astrocytes for 14 days at 37 °C and 5% CO_2. The culture medium was changed once per week. After 14 days adherent microglia were separated from astrocytes by adding PBS/EDTA and careful shaking. Purity of isolated microglia was more than 95%. Homogeneity of preparation was confirmed by flow

cytometric detection of murine microglial marker F4/80 (data not shown). After harvesting, microglial cells were seeded in well plates.

2.2.6. RNA Extraction and cDNA Synthesis

For quantification of mRNA, cells were seeded into 6-well plates and incubated at 37 °C (5% CO_2) overnight. Afterwards cells were disintegrated in Trizol reagent (Invitrogen Life Technologies; Darmstadt, Germany). Total RNA was extracted from Trizol as recommended by the manufacturer. To prevent contamination of mRNA preparation with chromosomal DNA, mRNA samples were treated with DNase. RNA amount and purity were determined by Nano-DropTM 1000 (Peqlab, Erlangen, Germany). For first strand cDNA synthesis, 1 μg total RNA was employed using the First Strand cDNA Synthesis Kit from Fermentas (St. Leon Rot, Germany). Synthesis was performed by the protocol recommended by the manufacturer.

2.2.7. Quantitative PCR

Quantitative PCR (qPCR) was performed with Maxima SYBR Green/ ROX qPCR Master Mix Kit (Fermentas; St. Leon Rot, Germany) containing Maxima Hot Start Taq DNA polymerase and appropriate primer pairs. The following primer pairs were used:

MMP-2 forward: TGGCAGTGCAATACCTGAAC and MMP-2 reverse: CCGTACTT-GCCATCCTTCTC,

MMP-3 forward: GTACCAACCTATTCCTGGTTGC and MMP-3 reverse: CCAGAGAG-TTAGATTTGGTGGG,

MMP-9 forward: ACCACTAAAGGTCGCTCGGATGGTT, MMP-9 reverse: AG-TACTGCTTGCCCAGGAAGACGAA,

MMP-13 forward: GGGCTCTGAATGGTTATGACATTC, MMP-13 reverse: AGCGCTCAGTCTCTTCACCTCTT,

GAPDH forward: CATGGCCTTCCGTGTTTCCTA and GAPDH reverse: CCTGCTTCACCACCTTCTTGAT.

Relative mRNA expression was calculated in relation to mRNA levels of the housekeeping gene, GAPDH, according to 2-ΔΔCT method (Livak and Schmittgen 2001).

2.2.8. *In Vitro* Chemotaxis Assay (Transwell migration assay)

To investigate the influence of lipid kinase dependent and -independent functions of PI3Kγ on microglial migration, transwell assays were performed. Cells were seeded in 6-well plates. After attachment, the cells were starved and incubated with serum-free medium overnight and then treated with LPS (100 ng/ml) for 24h. Following stimulation, 1×10^5 cells were transferred in 300 µl serum-free medium into the upper chamber of a 12-well chemotaxis insert (ThinCertTM, 8 µm pores; Greiner-Bio-One GmbH, Frickenhausen Germany). The chamber was placed in 700 µl serum-free medium containing chemoattractant (C5a; 10 ng/ml) and incubated at 37 °C (normal T_{Inc}) or at 33 °C (reduced T_{Inc}) with 5% CO_2 for 2 h. Afterwards cells on the lower side of the insert membrane were fixed with 100% ice-cold methanol and stained with 0.5% crystal violet solution (in 25% methanol) for 10 min. Average count of migrated cells was estimated through consideration of five independent visual fields.

2.2.9. *In Vivo* Microglial Migration Assay

Experiments were performed on adult (10-14 weeks) wild type, PI3Kγ$^{-/-}$, and PI3Kγ$^{KD/KD}$ mice (7 mice per group) kept during the whole experimental period at neutral T_a or reduced T_a, respectively. To investigate the effect of targeted PI3Kγ mutation on microglial migration, an *in vivo* wound healing experiment was performed. Mice were anesthetized by intraperitoneal injection of ketamine (100 mg/kg) and xylazine (16 mg/kg), and positioned in a stereotaxic apparatus (Stoelting, Wood Dale, IL, USA). Mice were then placed on a homeothermic heat blanket to maintain normal body temperature during surgery. The skull was exposed by a skin incision, and small burr holes were drilled through the skull. Using a micromanipulator focal stab, an injury was performed by gentle insertion of stainless steel pin (diameter 0.25 mm) into the parietal cortex at 3 mm below the dura mater (Schneble et al. 2017a; Seo et al. 2012). The pin was kept in place for two minutes and then removed. The burr holes were covered with bone wax, and the animals were returned to their cages. 12 h later, mice were deeply anesthetized and perfused with 4% paraformaldehyde (PFA) in phosphate buffer by cardiac puncture via the left ventricle. Brains were removed immediately after fixation and postfixed for 5 h in 4% PFA at 4 °C. After cryoprotection in PBS containing 30% sucrose, brains were frozen in methylbutane at -30 °C and stored at -80 °C.

Whole brains were cut by horizontal sections at 40 µm on a freezing microtome (Microm International GmbH, ThermoScientific, Germany). The slices were immunostained with anti-

Iba1 antibody to visualize microglia. Sections were photographed with a digital fluorescence camera (Nikon DSQi2), mounted on the Nikon inverted research microscope ECLIPSE Ti (NIKON INSTRUMENTS EUROPE B.V., Amstelveen, The Netherlands). Quantitative measurements (ImageJ software, National Institutes of Health, Bethesda, MD) blinded to the treatment groups were used to count cell numbers per voxel and expressed in mm^3. At the injured region, three voxels were predefined as follows: Voxel 1, a cylinder with a diameter of 400 μm, center lying in the middle of injury, and an altitude of 40 μm; Voxel 2, hollow cylinder, subsequently on Voxel 1, with an inner diameter of 400 μm, an outer diameter of 800 μm, and an altitude of 40 μm; Voxel 3, hollow cylinder, subsequently on Voxel 2, with an inner diameter of 800 μm, an outer diameter of 1200 μm, and an altitude of 40 μm. Number of Iba1-positive cells was counted in all three voxels. Migratory index was estimated as the ratio of cell number in Voxel 1 divided by the sum of cell number in Voxels 1, 2 and 3.

2.2.10. *In Vitro* Phagocytosis Assay

Efficiency of phagocytosis was investigated as previously described (Schneble et al. 2017a; Sun et al. 2008). Briefly, primary microglia cells obtained from wild type, PI3Kγ$^{-/-}$, and PI3Kγ$^{KD/KD}$ mice were seeded into 12-well plates on coverslips and incubated (37 °C, 5% CO_2) in microglia culture medium (10% FCS, 1% penicillin, 1% amphotericin B) and incubated at 37 °C (5% CO_2) for 24 h. Coverslips were coated 2 h by Poly-L-Lysine (25 μg/ml) at 37 °C before use. After attachment cells were starved for 24 h in DMEM without FCS. Cells were subsequently stimulated with LPS (100 ng/ml). Phagocytosis assay was performed by using fluoresceinisothiocyanate (FITC)-labeled Zymosan A S. cerevisiae BioParticles (9800 per μl) (# Z2841, Thermo Fisher Scientific, Waltham, USA). 7 μl of the suspended particles was added to the microglial cells and incubated 1 h at either 37 °C or 33 °C. After incubation the cells were fixed with 4% PFA, washed three times and stained with DAPI–solution for 5 min (1:1000 in PBS). Phagocytosed particles and cells of five independent visual fields were counted under a fluorescence microscope. The result of the phagocytosis of primary microglia was calculated by determining the phagocytic index (the uptake rate of FITC-Zymosan particles per cell).

2.2.11. *In Vivo* Phagocytosis Assay

Experiments were performed on adult (10-14 weeks) wild type, PI3K$\gamma^{-/-}$, and PI3K$\gamma^{KD/KD}$ mice (7 mice per group) kept during the whole experimental period at neutral T_a or reduced T_a, respectively. To investigate the effect targeted PI3Kγ mutation on microglial phagocytosis FITC-labeled Zymosan particles (9800 per µl) were administered into the brain as described previously (Schmidt et al. 2013). Briefly, mice were anesthetized by intraperitoneal injection of ketamine (100 mg/kg) and xylazine (16 mg/kg), and positioned in a stereotaxic apparatus (Stoelting, Wood Dale, IL, USA). The skull was exposed by a skin incision, and small burr holes were drilled through the skull. Using a micromanipulator a cannula (diameter 0.24 mm) attached on a Hamilton microsyringe (10 µl) was stereotaxically placed into the parietal cortex on both sides (stereotaxic coordinates were AP, -2.0 mm; L, ±0.5 mm; and V, -2.5 mm, respectively (Paxinos and Franklin 2001)). Subsequently, 4 µl of FITC-labeled Zymosan particles suspended in artificial cerebrospinal fluid were infused within 120 seconds. The cannula remained in place for 5 minutes before removal. Twenty-four hours later mice were deeply anesthetized and perfused with 4% PFA in phosphate buffer by cardiac puncture via the left ventricle. Brains were removed immediately after fixation and post-fixed for 5 h in 4% PFA at 4 °C. After cryoprotection in PBS containing 30% sucrose, brains were frozen in methylbutane at -30 °C and stored at -80 °C. Whole brains were cut by coronal sections at 40 µm on a freezing microtome (Microm International GmbH, Thermo Scientific, Germany). The slices were immunostained with anti-Iba1 antibody to visualize microglia. A voxel with an edge length of 400 µm, and an altitude of 40 µm were predefined as region of interest. Z-stack imaging was performed with a 20x objective using a digital fluorescence camera (Nikon DS-Qi2), mounted on the Nikon inverted research microscope ECLIPSE Ti (NIKON INSTRUMENTS EUROPE B.V., Amstelveen, The Netherlands). Quantitative measurements (ImageJ software, National Institutes of Health, Bethesda, MD) blinded to the treatment groups were used to count the percentage number of Iba-1 positive cells per mm^3 containing Zymosan particles.

### 2.2.12. Histopathology and immunohistochemistry

For determination of microglial activation, PMN homing, MMP-9 expression and terminal deoxynucleotidyl transferase dUTP nick end labeling (TUNEL) positivity brains were fixated in situ by transcardial perfusion with 4% PFA after rinsing with PBS. Afterwards, they were immediately removed after fixation, post-fixated in 4% PFA at 4 °C for 1 day, embedded in

paraffin and cut into 6-µm-thick sections. After deparaffinization, the sections were heated with citrate buffer (0.01 M, pH6.0) in the microwave (630 W, 11min) for antigen removal and the nonspecific binding sites were blocked with blocking solution (5% NDS, 1% BSA-c, PBST). Then the slide-mounted tissue sections were incubated with the desired primary antibody in antibody incubation solution (5% NDS, 1% BSA-c, PBST) at 4 °C overnight, followed by an incubation with the associated secondary antibody at 4 °C for 1 h. Negative control sections were incubated with goat serum in absence of the primary antibody. The following primary antibodies were used: goat polyclonal anti-Iba-1 (1:250) antibody (Abcam, Cambridge, UK) for Iba1 staining, rabbit polyclonal anti-MMP-9 (1:150) antibody (Cell Signaling Technology, Danvers, USA) for MMP-9 and rabbit anti-mouse PMN (ACCURATE CHEMICAL & SCIENTIFIC CO, USA) for neutrophils staining. For visualization, the secondary fluorescent goat anti-mouse isotype-specific antibody Alexa Fluor® 488 (Molecular Probes, Inc., Eugene, USA), donkey anti-goat IgG antibody Alexa Fluor®568 (Thermo Fisher Scientific, Waltham, USA) were used. Method for TUNEL staining was described elsewhere (Brodhun et al. 2001). Briefly, sections were deparaffinized and prepared for TUNEL-staining. Fragmented DNA was detected in situ by the TUNEL method using a commercially available kit according to the manufacturer's protocol (In Situ Cell Death Detection Kit, POD; Roche, Germany). Deparaffinized sections were pretreated with 20 mg/ml proteinase K and washed in PBS prior to TUNEL staining. TUNEL staining was performed by incubation with fluorescein-conjugated digoxigenin-UTP and terminal deoxynucleotidyltransferase at 37 °C for 1 h. DNA fragmentation was visualized using converter-alkaline phosphatase, NBT/BCIP and counterstaining with Kernechtrot.

Assessment of microglial activation after LPS-induced SIRS were performed by use of morphological criteria, as previously described (Kettenmann et al. 2011; Zhang et al. 2008).

Stained brain sections were visualized by fluorescence imaging. Iba-1 positive cells, which had a clear nucleus, were included in the analysis. Three randomly sampled areas from frontal cortex, hippocampus and thalamus were examined. The percentage of a particular cell type (ramified or polarized, Fig.3) was obtained by calculating the ratio of the cell number of this type to the total number of microglial cells examined per section.

Cell counting as well as estimation of migration and phagocytic index were performed blinded for genotype and treatment. In each case evaluation was performed on three different slices obtained from frontal cortex, thalamus and hippocampus, each. Five separate fields of vision were counted with at least 100 cells each.
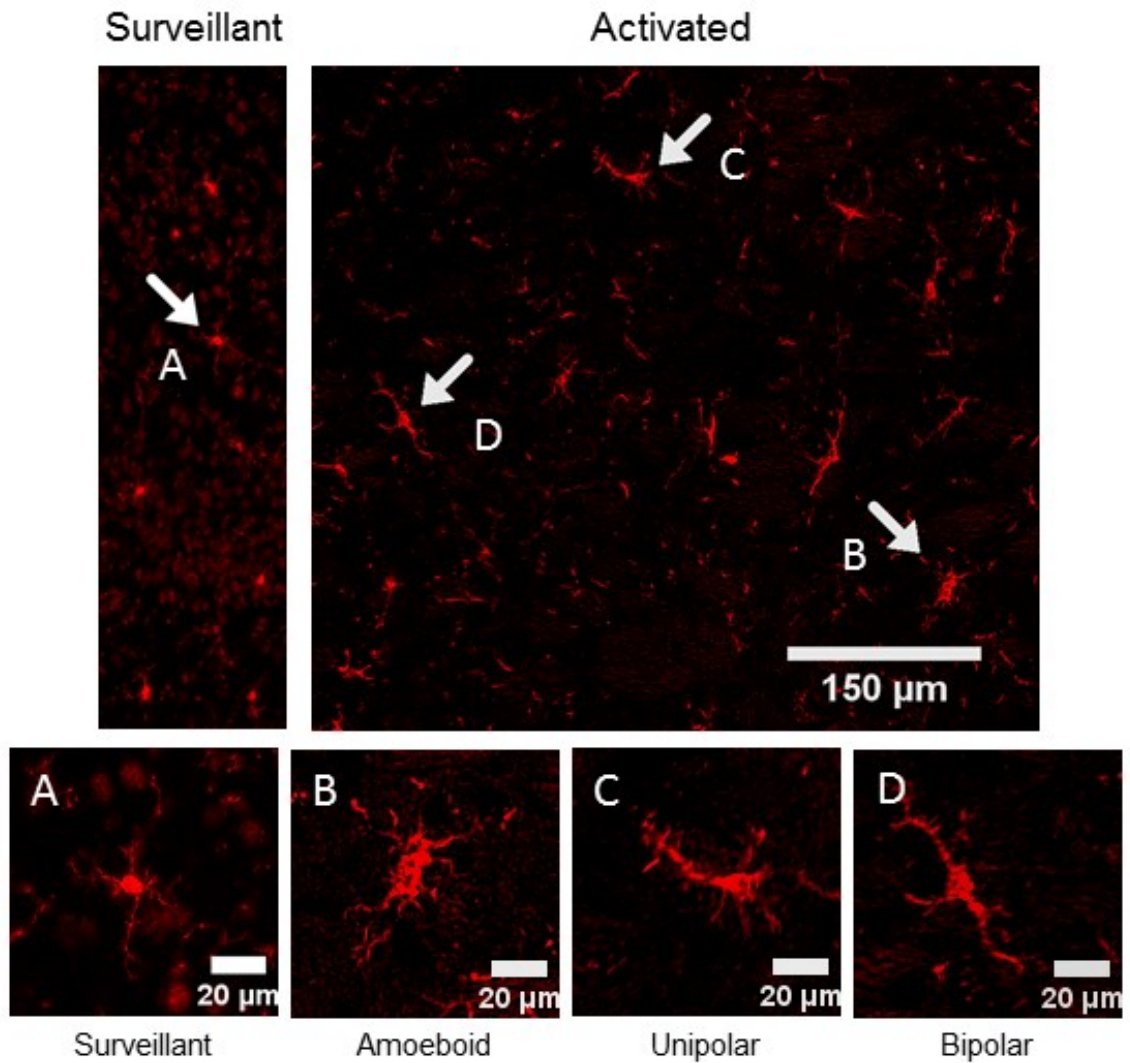
Figure 3. Morphology of surveillant ("resting") and activated microglia.

Iba-1 positive cells were assessed as brain microglial cells. They were classified as ramified (A), amoeboid (B), unipolar (C) and bipolar (D). Ramified microglial cells are defined by thin, slender, radially projecting processes with well-developed ramifications. Amoeboid microglial cells are defined as having large soma, and short, thick and radially projecting processes. Unipolar and bipolar microglial cells were defined as having one or two thick process with well-developed ramifications.

2.2.13. Cell metabolism measurement

OCR (oxygen consumption rate) and ECAR (extracellular acidification rate), as indicators of cellular oxidative phosphorylation and glycolysis, respectively, were monitored consecutively with a Sea-horse Bioscience extracellular flux analyzer (XF96, Seahorse Bioscience) as described previously (Gerencser et al. 2009). Approximately 20×10^3 cells were seeded on 96-well Seahorse XF96 microplates. Cells were starved and treated with LPS (100 ng/ml) for 24h at different temperatures (33 °C and 37 °C). Before the experiment, cell supernatants were re-

placed by Agilent Seahorse XF Assay Medium, pH 7.4, supplemented with 10 mM D-glucose (Sigma Aldrich, Germany) and 1 mM sodium pyruvate (Thermo Fisher Scientific, Germany). Cells were then cultured for one hour in a CO_2-free incubator at 37 or 33 °C. OCR and ECAR were monitored at basal conditions as pmoles/min and mpH/min respectively, in cycles of 3 min mix and 3 min measure at 37 or 33 °C in six replicates per condition. All values were normalized to exact cell numbers, which was measured by high-content microscopy. For that purpose, cell supernatants were removed from the 96-well Seahorse XF96 microplate and cells were 10 min fixed with 100% methanol at room temperature. Cells were then washed once with PBS and incubated for 10 min with 1 µg/ml DAPI at room temperature. After two more washing steps with PBS, cell nuclei were counted on an ImageXpress Micro confocal high-content imaging system (Molecular Devices).

2.2.14. Statistics

The statistical analysis was performed using SigmaPlot Software (Sigma-Plot Software, San Jose, USA). All data are presented as boxplots illustrating medians within boxes from first quartile (25th percentile) to the third quartile (75th percentile) and whiskers ranging from the 10th to the 90th percentiles (extreme values are marked outside). Numbers of animals are given in figure legends for each group and time point. Comparisons between groups were made with one-way or two-way analysis of variance, if appropriate. In case of repeated measurements, one-way and two-way analysis of variance with repeated measures was used, if appropriate. Post hoc comparisons were made with the Holm-Sidak test or t-tests with Bonferroni's correction for adjustments of multiple comparisons. Data not following normal distribution was tested with Kruskal-Wallis test followed by Dunn's multiple comparisons test.

3. Results

3.1. Impact of ambient temperature on degree of SIRS and SIRS-induced BBB disturbance

Intraperitoneal LPS administration (10 mg/kg) induced a robust and similarly distinct SIRS in mice kept under neutral as well as reduced T_a and mainly independent from genetic status, as revealed by corresponding cytokine release in blood plasma and brain tissue (Tab. 5). However, reduced T_a induced a moderately worsened sickness state in PI3Kγ-deficient mice (Tab. 6).
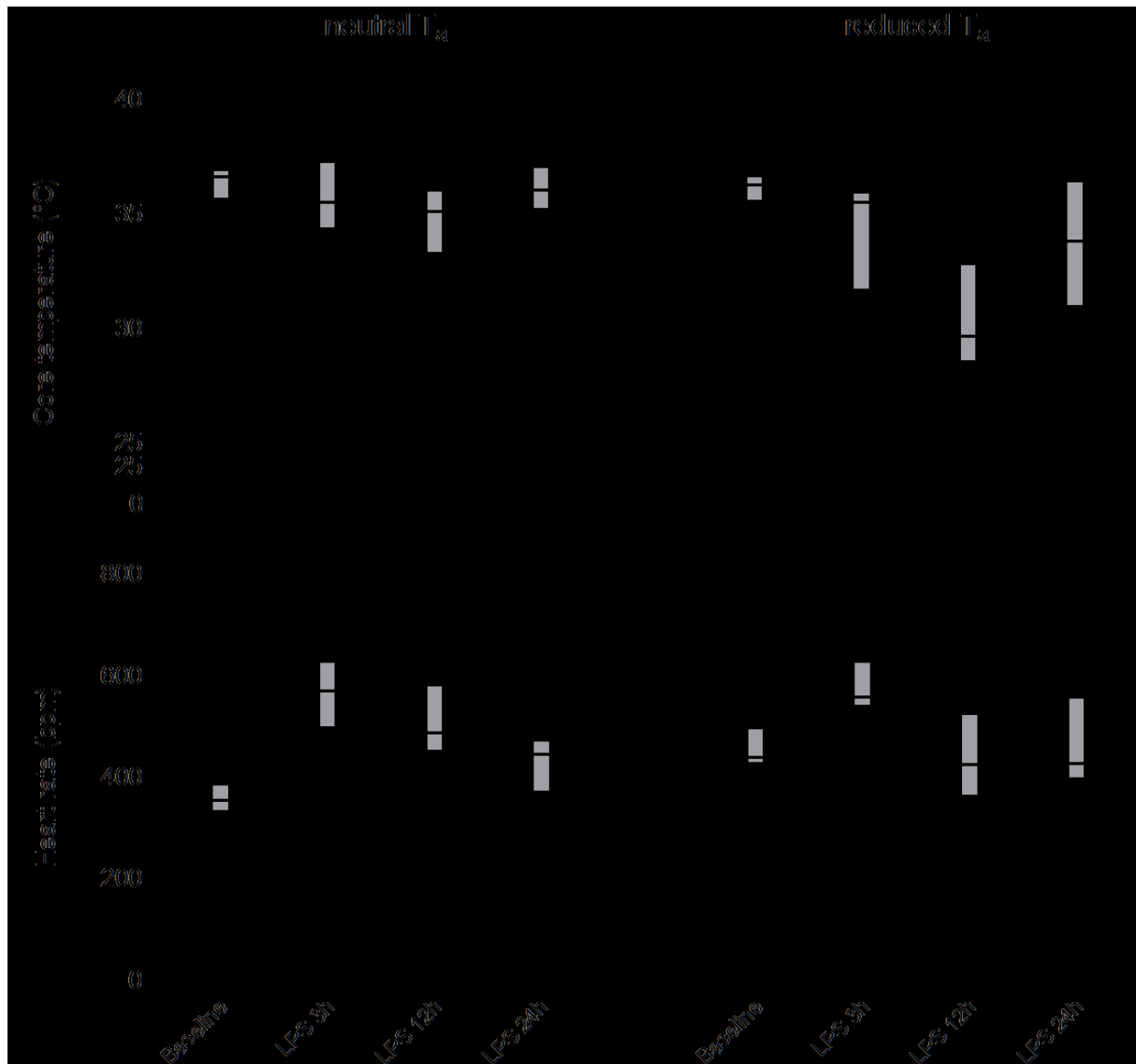
Figure 4. Influence of T_a on heart rate and hypothermia.

Enhanced heart rate and augmented hypothermia in mice kept under reduced ambient temperature (T_a) after LPS-induced SIRS response compared with mice kept under neutral T_a irrespective of the genotype (wild-type mice, open boxplots, PI3Kγ-deficient mice (PI3Kγ$^{-/-}$) filled boxplots, PI3Kγ-kinase-dead mice (PI3Kγ$^{KD/KD}$) hatched boxplots).Values are presented as boxplots illustrating medians within boxes from first quartile to the third quartile, whiskers ranging from the 10th to the 90th percentiles (neutral T_a groups: wild type mice n=9, PI3Kγ$^{-/-}$ n=10, PI3Kγ$^{KD/KD}$, n=8; reduced T_a groups: wild type mice n=12, PI3Kγ$^{-/-}$ n=10, PI3Kγ$^{KD/KD}$ n=9). *† p < 0.05, * signifi-

cant difference between baseline and LPS stimulation within each T_a state, [†] significant differences versus mice kept under neutral T_a (two-way repeated measures ANOVA, followed by Holm-Sidak test for post hoc multiple comparisons were performed).

Telemetric T_c monitoring revealed that under baseline conditions all mice kept under neutral as well as reduced T_a showed no differences in body temperature. However, reduced T_a was obviously accompanied by an enhanced sympathetic tone to the heart already under baseline condition, indicated by a markedly increased HR regardless of the genotype (Fig. 4).
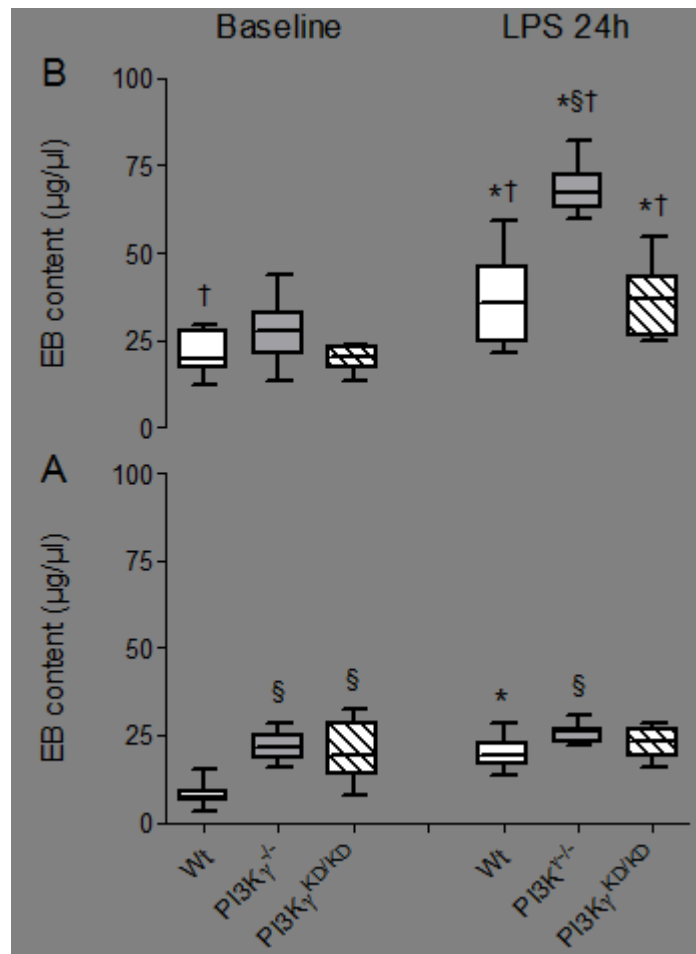
Figure 5. Influence of T_a on BBB integrity.

Enhanced BBB leakage by PI3Kγ-deficiency at reduced T_a at LPS induced SIRS. (A) Mild disturbance of BBB integrity in PI3Kγ mutant mice kept under neutral T_a. LPS-induces SIRS elicit small increase of BBB leakage in wild type mice (Wt, open boxplots). (B) Reduced T_a was accompanied by enhanced Evans blue (EB) extravasation into brain tissue indicating degree of BBB leakage in PI3Kγ-deficient (PI3Kγ$^{-/-}$) mice (filled columns) in comparison with Wt and kinase-dead (PI3Kγ$^{KD/KD}$, hatched boxplots) mice. Values are presented as boxplots illustrating medians within boxes from first quartile (25th percentile) to the third quartile (75th percentile) and whiskers ranging from minimum to maximum, n=10 per group and time point. * [†] [§] $p < 0.05$, * significant differences versus baseline conditions within the same genotype, [†] significant differences versus neutral T_a within the same genotype, [§] significant differences versus Wt mice within the same T_a condition (Two-way ANOVA and one-way ANOVA, followed by Holm-Sidak test for post hoc multiple comparisons was performed for comparison between respected groups, t-test was used for comparisons between states within same groups with Bonferroni's correction for adjustments of multiple comparisons)

Table 5. Cytokine content in blood plasma and brain tissue

Cytokine content		Baseline	LPS 3h	LPS 24h
Blood plasma				
TNFα (ng $\cdot$ ml^{-1})				
neutral T$_a$	Wt	4.9 (4.8; 5.4)	2329 (2081; 2755)*	5.7 (5.7; 7.9)
	PI3K$\gamma^{-/-}$	4.1 (4.1; 4.6)	2951 (2741; 3066)*	6.1 (4.7; 7.7)
	PI3K$\gamma^{KD/KD}$	3.0 (2.8; 4.5)	1322 (1182; 1368)*	3.5 (3.6; 4.0)
reduced T$_a$	Wt	6.3 (5.4; 6.5)	1892 (1767; 2105)*	3.4 (3.2; 5.1)
	PI3K$\gamma^{-/-}$	4.7 (4.6; 5.6)	1580 (1530; 1597)*	5.9 (5.5; 6.0)
	PI3K$\gamma^{KD/KD}$	4.8 (3.7; 4.9)	1190 (1169; 1512)*§	6.3 (5.3; 8.5)
Il6 (ng $\cdot$ ml^{-1})				
neutral T$_a$	Wt	4.2 (3.8; 4.6)	101277 (94178; 134250)*	494 (469; 529)*
	PI3K$\gamma^{-/-}$	3.4 (3.3; 3.4)	77147 (69520; 92818)*§	451 (412; 549)*
	PI3K$\gamma^{KD/KD}$	3.0 (2.9; 3.1)	37417 (32741; 45597*§	296 (281; 401)*
reduced T$_a$	Wt	6.0 (4.9; 10.8)	81446 (73249; 105982)*	444 (381; 541)*
	PI3K$\gamma^{-/-}$	3.5 (3.5; 8.6)	68946 (60700; 71937)*	404 (368; 514)*
	PI3K$\gamma^{KD/KD}$	3.1 (3.0; 3.3)	55578 (48955; 71880)*§	207 (178; 249)*
MCP-1 (ng $\cdot$ ml^{-1})				
neutral T$_a$	Wt	14.1 (13.7; 24.1)	77811 (69094; 90783)*	6468 (6427; 6493)*
	PI3K$\gamma^{-/-}$	7.7 (6.8; 7.9)	71915 (69727; 79884)*	6160 (5048; 6176)*
	PI3K$\gamma^{KD/KD}$	6.8 (3.8; 7.9)	49375 (41716; 59061)*†§	3994 (3407; 5077)*
reduced T$_a$	Wt	12.4 (9.8; 13.7)	49757 (44674; 62181)*†	1733 (1564; 2236)*
	PI3K$\gamma^{-/-}$	3.8 (1.9; 6.0)	41911 (39677; 43170)*	3250 (2483; 3456)*
	PI3K$\gamma^{KD/KD}$	8.1 (5.5; 8.5)	38229 (36030; 48311)*	5940 (5879; 6727)*
Brain tissue				
TNFα (ng $\cdot$ g^{-1})				
neutral T$_a$	Wt	2.4 (1.7; 2.4)	10.5 (8.5; 11.0)*	2.5 (2.5; 2.7)
	PI3K$\gamma^{-/-}$	2.8 (2.6; 3.3)	11.4 (10.4; 12.5)*§	3.0 (1.8; 4.3)
	PI3K$\gamma^{KD/KD}$	2.0 (1.8; 2.9)	8.3 (7.8; 8.9)*§	7.5 (4.8; 9.9)
reduced T$_a$	Wt	2.4 (1.8; 2.5)	26.3 (25.0; 27.6)*†	2.7 (2.6; 4.0)
	PI3K$\gamma^{-/-}$	2.5 (2.1; 2.6)	12.0 (9.5; 28.1)*†§	4.9 (4.3; 7.7)
	PI3K$\gamma^{KD/KD}$	2.7 (1.7; 2.9)	10.6 (7.9; 11.8)*§	9.7 (6.0; 14.6)
Il6 (ng $\cdot$ g^{-1})				
neutral T$_a$	Wt	2.8 (2.8; 3.0)	471 (427; 602)*	9.8 (9.3; 10.2)*
	PI3K$\gamma^{-/-}$	3.5 (3.3; 3.7)	367 (356; 378)*§	10.9 (9.7; 12.6)*
	PI3K$\gamma^{KD/KD}$	2.6 (2.6; 2.9)	226 (218; 233)*§	17.4 (15.8; 21.8)*
reduced T$_a$	Wt	3.4 (2.8; 3.4)	406 (386; 426)*†	20.5 (20.5; 21.7)*
	PI3K$\gamma^{-/-}$	1.9 (1.9; 2.7)	270 (266; 408)*	14.2 (11.8; 15.4)*
	PI3K$\gamma^{KD/KD}$	3.4 (3.0; 3.4)	153 (143; 163)*†§	21.5 (19.5; 26.5)*
MCP-1 (ng $\cdot$ g^{-1})				
neutral T$_a$	Wt	17.7 (15.7; 22.0)	1038 (1001; 1179)*	333 (296; 336)*
	PI3K$\gamma^{-/-}$	13.2 (12.1; 17.9)	1102 (1095; 1110)*	228 (222; 266)*
	PI3K$\gamma^{KD/KD}$	24.2(20.6; 26.9)	1049 (986; 1112)*	468 (354; 483)*
reduced T$_a$	Wt	12.8 (12.4; 14.6)	1068 (1015; 1122)*	317 (266; 383)*
	PI3K$\gamma^{-/-}$	17.1 (12.4; 17.0)	908 (877; 1040)*	368 (288; 408)*
	PI3K$\gamma^{KD/KD}$	14.9 (12.4; 20.7)	637 (616; 856)*†§	247 (243;327)*

(Values are given as medians as well as the first quartile and third quartile in parenthesis, *† § $p < 0.05$, * significant differences versus baseline conditions within the same genotype, † significant differences versus neutral T$_a$ within the same genotype, § significant differences versus wild type (Wt) mice within the same T$_a$ condition).

Figure 5 reveals a small BBB breakdown 24 hours after LPS administration in PI3Kγ-deficient and PI3Kγ-kinase-dead mice, when housed under neutral T_a. Additional LPS-induced SIRS provoked an increase of BBB leakage in wild type mice, whereas PI3Kγ-deficient mice exhibited a small but significantly enhanced BBB disturbance compared with wild type mice. In contrast, housing under reduced T_a induced BBB breakdown in wild type mice at a similar degree as ascertained in the mutant mice (Fig 5B). Additional LPS-induced SIRS provoked a substantially enhanced BBB breakdown, which was most pronounced in PI3Kγ-deficient mice. Of note, lipid kinase-dead mutant mice display similar degree of BBB breakdown as wild type mice indicating a causal impact of lipid kinase independent PI3Kγ signaling on the verified phenotypes.

**Table 6. Clinical severity score (according to Gonnert et al 2011).**

	Baseline	*24h-LPS*
Neutral T_a		
Wt	1.0 (1.0; 1.0)	1.5 (1.0; 2.0)*
PI3Kγ$^{-/-}$	1.0 (1.0; 1.0)	2.0 (1.5; 2.0)*
PI3Kγ$^{KD/KD}$	1.0 (1.0; 1.0)	1.0 (1.0; 2.0)*
Reduced T_a		
Wt	1.0 (1.0; 1.0)	2.0 (1.5; 2.0)*
PI3Kγ$^{-/-}$	1.0 (1.0; 1.0)	2.5 (2.0; 3.0)*[†§]
PI3Kγ$^{KD/KD}$	1.0 (1.0; 1.0)	2.0 (2.0; 2.0)*[†]

(Values are given as medians as well as the first quartile and third quartile in parenthesis, n=4-6 animals at each group and experimental state. * [§] †$p < 0.05$, * significant difference between baseline and LPS-stimulated state within each group, [§] significant difference versus wild type (Wt) mice kept under same ambient temperature, †significant differences versus mice kept under neutral ambient temperature).

3.2. Impact of T_a dependent BBB disturbance on degree of microglial activation, MMP expression, apoptosis, and PMN invasion

To verify consequences of LPS-induced BBB disturbance, extent of neuroinflammation was assessed by different approaches. First we quantified the number of activated microglial cells assessed by shape characteristics (Kettenmann et al. 2011; Zhang et al. 2008). As shown in Fig. 6, a marked increase in microglial cell number with altered, mainly polarized shape occurred. Analysis of regional distribution revealed similarity in extent of microglial cell activation in brain cortex, hippocampus and thalamus (Tab. 7) suggesting a diffuse microglial activation due to LPS-induced SIRS. Though, a significant genotype related effect could not be emerged. In

contrast, MMP expression in brain tissue obtained 24 hours after LPS injection displayed significant PI3Kγ dependency.
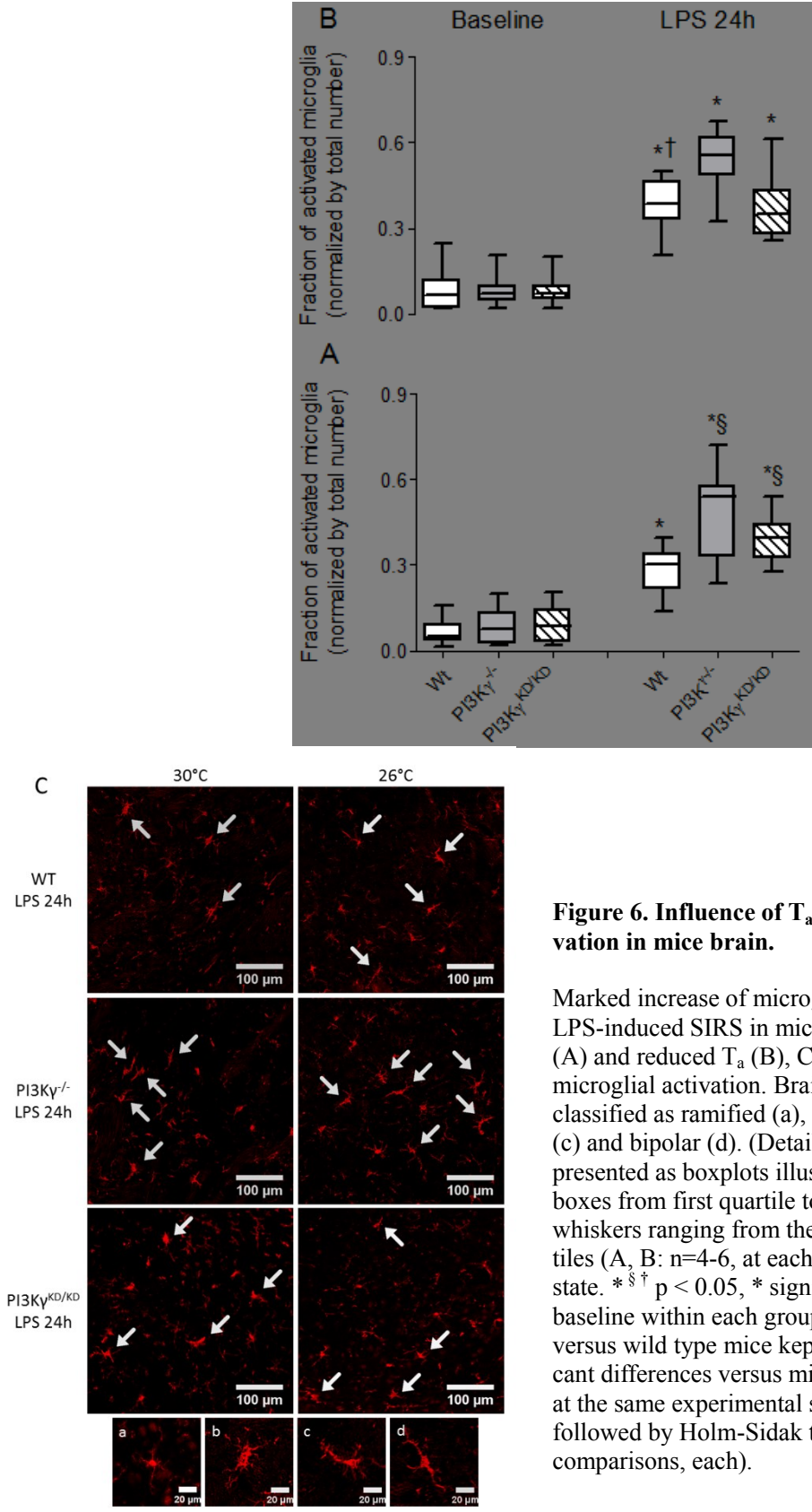
Figure 6. Influence of T_a on microglial cell activation in mice brain.

Marked increase of microglial cell activation by LPS-induced SIRS in mice kept under neutral T_a (A) and reduced T_a (B), C: representative images of microglial activation. Brain microglial cells were classified as ramified (a), amoeboid (b), unipolar (c) and bipolar (d). (Details see 2.2.12). Values are presented as boxplots illustrating medians within boxes from first quartile to the third quartile and whiskers ranging from the 10th to the 90th percentiles (A, B: n=4-6, at each group and experimental state. $*^{§†}$ p < 0.05, * significant difference between baseline within each group, $§$ significant differences versus wild type mice kept under same T_a, $†$ significant differences versus mice kept under neutral T_a at the same experimental state, two-way ANOVA, followed by Holm-Sidak test for post hoc multiple comparisons, each).

Table 7. Quantitative analysis of cell density of activated microglia (assessed by cell shape characteristics) in different brain structures

Groups	Cortex		Hippocampus		Thalamus	
	Baseline	*24h-LPS*	*Baseline*	*24h-LPS*	*Baseline*	*24h-LPS*
Neutral T_a						
Wt	0.04 (0.03, 0.04)	0.28 (0.2, 0.36) *	0.06 (0.05, 0.07)	0.27 (0.22, 0.33) *	0.09 (0.05, 0.09)	0.3 (0.28, 0.31) *
PI3Kγ$^{-/-}$	0.05 (0.02, 0.08)	0.4 (0.28, 0.51) *	0.05 (0.03, 0.09)	0.5 (0.4, 0.56) *§	0.15 (0.12, 0.18)	0.6 (0.58, 0.65) *§
PI3Kγ$^{KD/KD}$	0.04 (0.03, 0.06)	0.32 (0.3, 0.35) *	0.06 (0.03, 0.12)	0.42 (0.39, 0.44) *	0.12 (0.09, 0.16)	0.41 (0.36, 0.47) *
Reduced T_a						
Wt	0.03 (0.02, 0.09)	0.39 (0.3, 0.43) *	0.04 (0.02, 0.09)	0.38 (0.33, 0.38) *	0.13 (0.05, 0.19)	0.46 (0.44, 0.48) *†
PI3Kγ$^{-/-}$	0.05 (0.04, 0.06)	0.51 (0.38, 0.38) *	0.06 (0.05, 0.08)	0.55 (0.5, 0.5) *§	0.09 (0.08, 0.11)	0.61 (0.53, 0.63) *
PI3Kγ$^{KD/KD}$	0.06 (0.04, 0.08)	0.33 (0.28, 0.34) *	0.07 (0.06, 0.09)	0.35 (0.28, 0.42) *	0.1 (0.07, 0.1)	0.43 (0.39, 0.43) *

(Values are given as medians as well as the first quartile and third quartile in parenthesis, n=4-6 animals at each group and experimental state. * § †p < 0.05, * significant difference between baseline and LPS-stimulated state within each group, § significant difference versus wild type (Wt) mice kept under same ambient temperature, †significant differences versus mice kept under neutral ambient temperature).

There was an enhanced RNA expression in brains obtained from PI3Kγ-deficient mice kept under reduced T_a in all MMPs under consideration compared to mice kept under neutral T_a (Fig. 7). Furthermore, there was an increased mRNA expression in brains derived from PI3Kγ–deficient mice kept under reduced T_a compared with wild type mice kept under same housing conditions. In contrast, PI3Kγ$^{KD/KD}$ mice showed a similar response as wild type mice suggesting a lipid kinase independent mode of action. Increased cerebral MMP expression appeared apparently as a result of reinforced microglial activation in PI3Kγ$^{-/-}$ mice kept under reduced T_a shown by an increased number of MMP-9 positive cells co-expressed in Iba-1 positive cells in these brains (Fig. 8). Analysis of regional distribution revealed similarity in the extent of microglial MMP-9 expression in brain cortex, hippocampus and thalamus (Tab. 4).
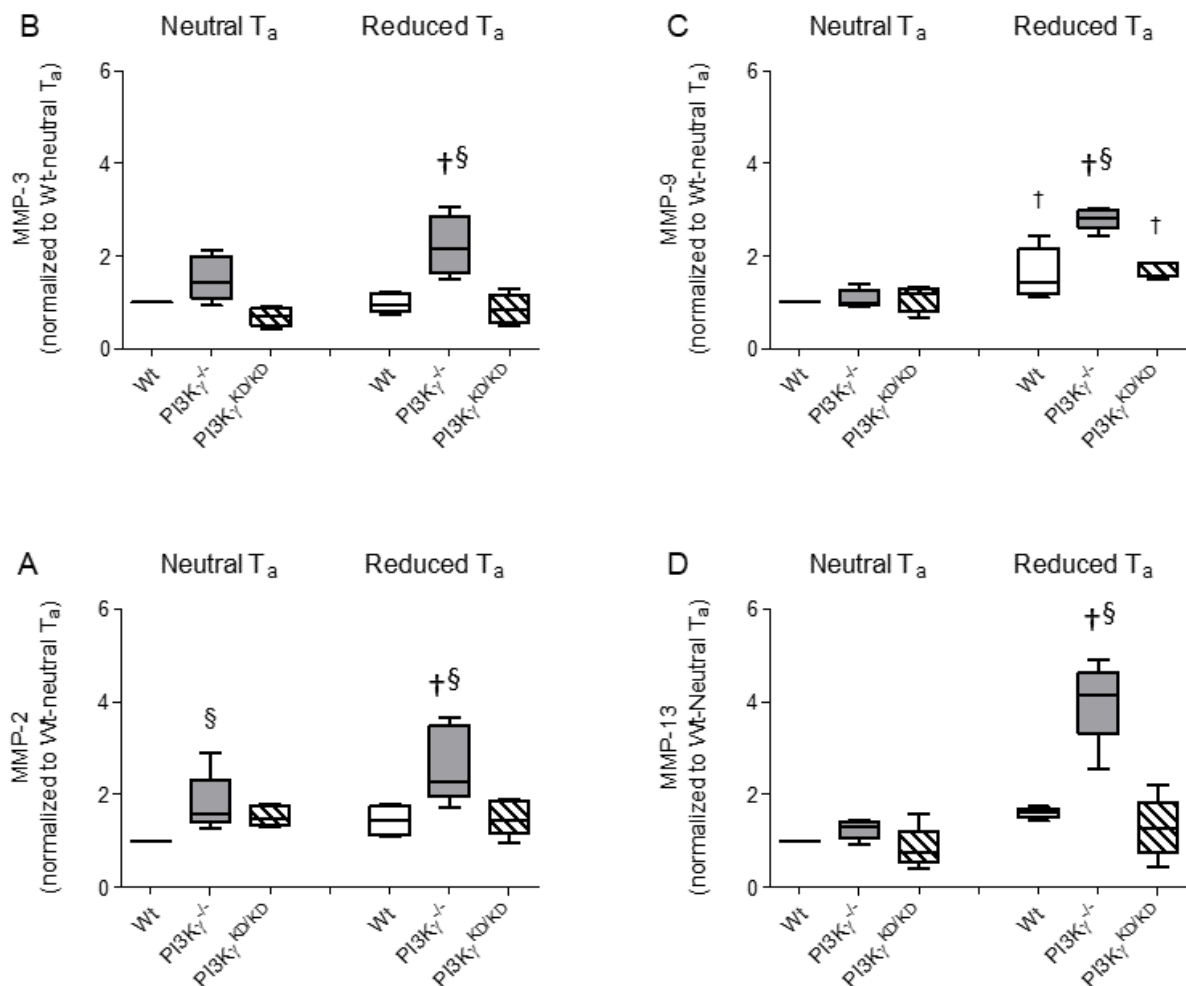
Figure 7. Influence of T_a on MMPs mRNA expression in mice brain.

Increased LPS-induced mRNA expression of MMP-2, MMP-3, MMP-9, and MMP-13 appeared mainly in brains obtained from PI3Kγ-deficient mice kept under reduced T_a. Values are presented as boxplots illustrating medians within boxes from first quartile to the third quartile and whiskers ranging from the 10th to the 90th percentiles (A-D n=5 at each group and experimental state. §† $p < 0.05$, § significant differences versus wild type mice kept under same T_a, † significant differences versus mice kept under neutral T_a at the

same experimental state, two-way ANOVA, followed by Holm-Sidak test for post hoc multiple comparisons, each).
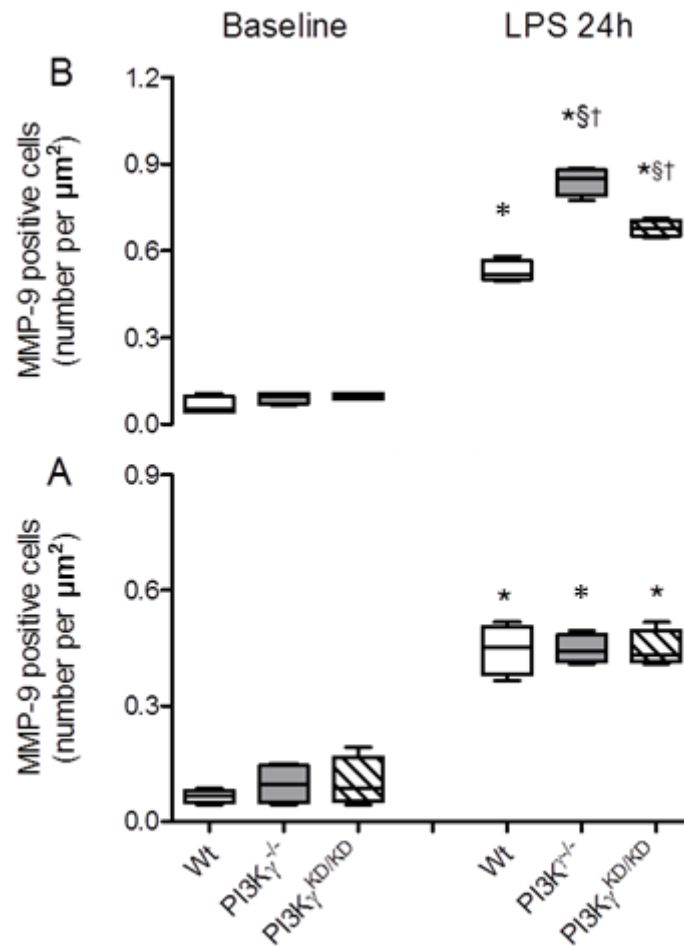
Figure 8. Influence of T_a on microglial MMP-9 expression.

Increased number of MMP-9 positive microglial cells in brains obtained from PI3Kγ$^{-/-}$ and PI3Kγ$^{KD/KD}$ mice kept under reduced T_a (B) compared to mice kept under neutral T_a (A) 24h after LPS administration. C: representative images of microglial activation (see next page). Values are presented as boxplots illustrating medians within boxes from first quartile to the third quartile and whiskers ranging from the 10th to the 90th percentiles (lower panel: neutral T_a, upper panel: reduced T_a, n=4 at each group and experimental state. * § † $p < 0.05$, * significant differences versus baseline at the same genotype and experimental state, § significant differences versus wild type mice kept under same T_a, † significant differences versus mice kept under neutral T_a at the same experimental state, two-way ANOVA, followed by Holm-Sidak test for post hoc multiple comparisons, each).

C

WT | PI3Kγ^{−/−} | PI3Kγ[KD/KD]

Iba1 | MMP9 | Merge

Neutral Ta baseline
Reduced Ta baseline
Neutral Ta LPS
Reduced Ta LPS
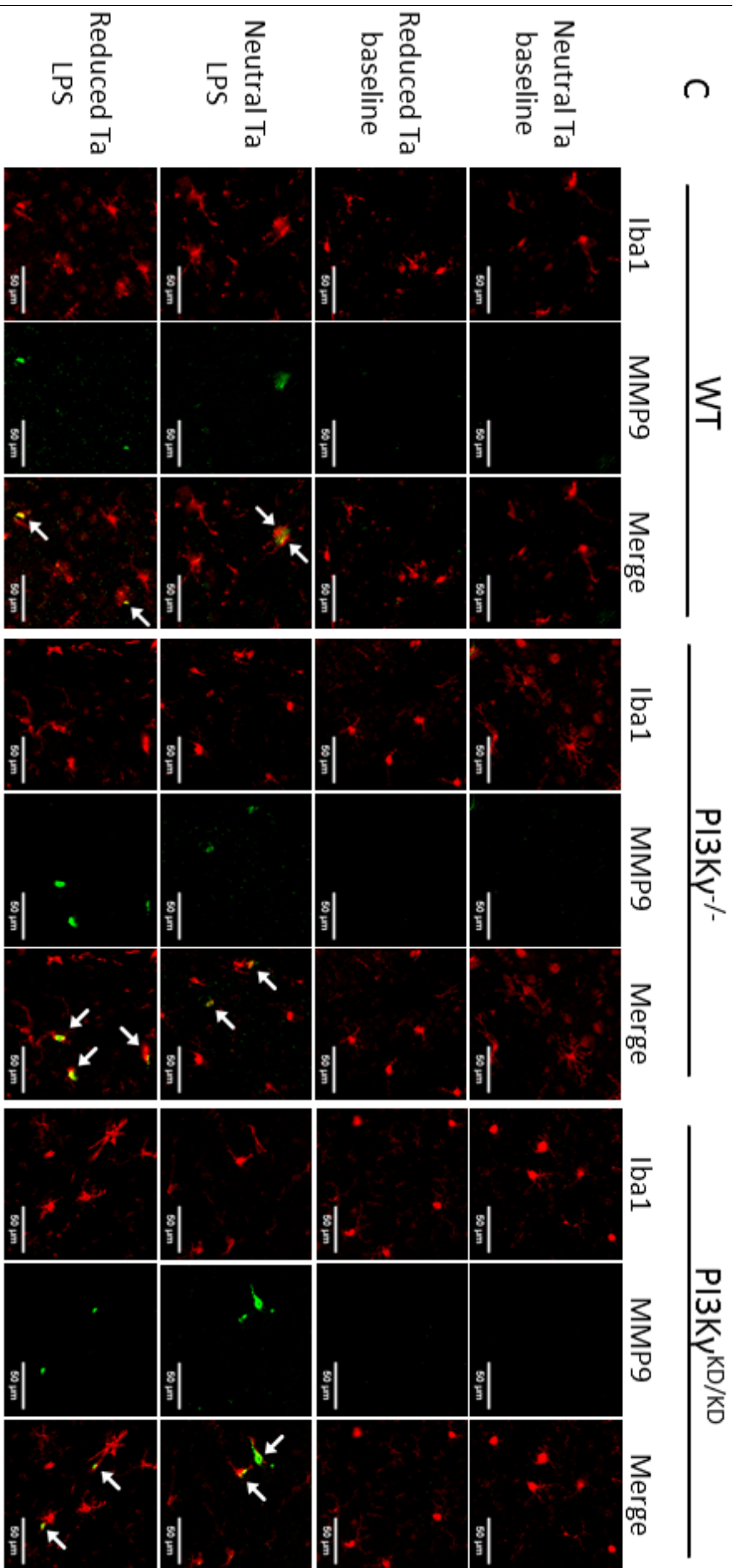
To examine a possible T_a-dependent impact of LPS-induced BBB leakage on structural integrity of brain tissue, we quantified the extent of apoptosis in brain slices derived from wild type, PI3K$\gamma^{-/-}$, and PI3K$\gamma^{KD/KD}$ mice kept under neutral and reduced T_a. Already under baseline conditions the rate of apoptotic cells was significantly increased in brains of PI3K$\gamma^{-/-}$ mice kept under reduced T_a compared with those kept at neutral T_a. LPS-induced SIRS exhibited always an increased number of apoptotic cells, which was most pronounced in PI3K$\gamma^{-/-}$ mice kept under reduced T_a (Fig. 9).
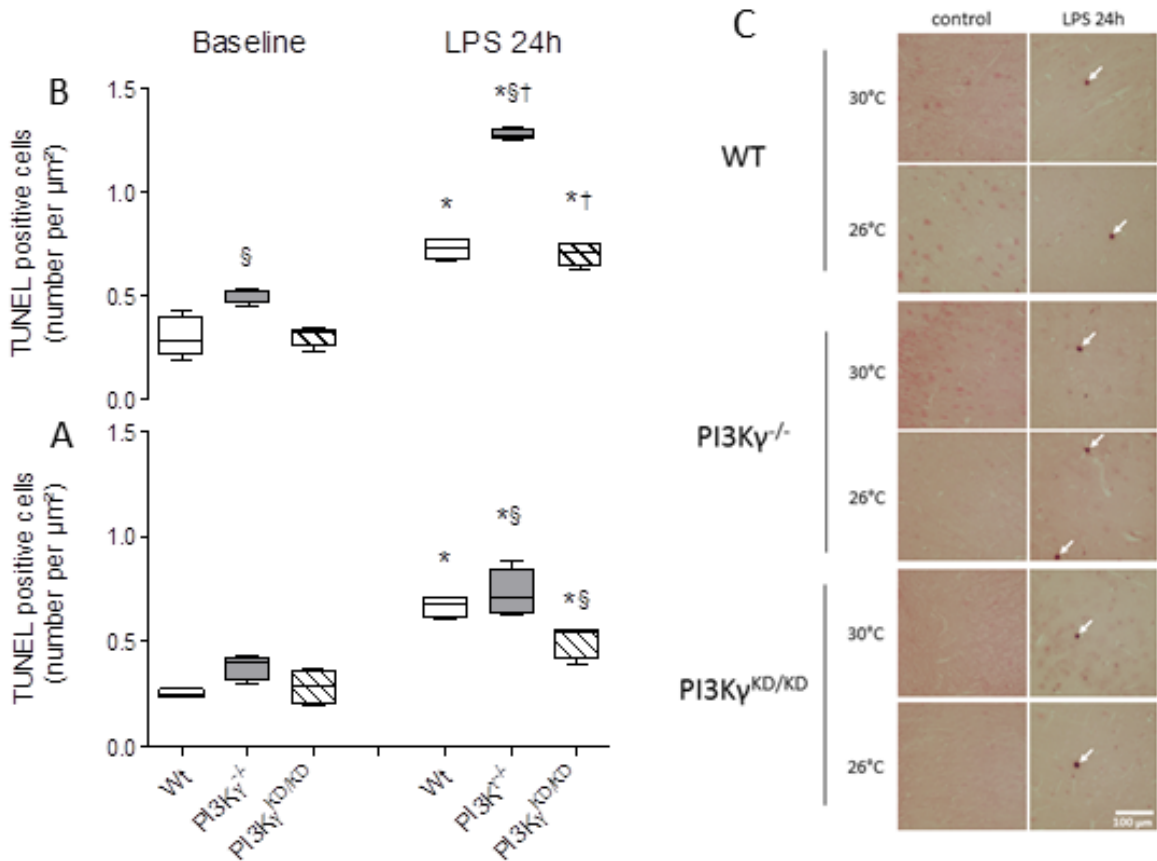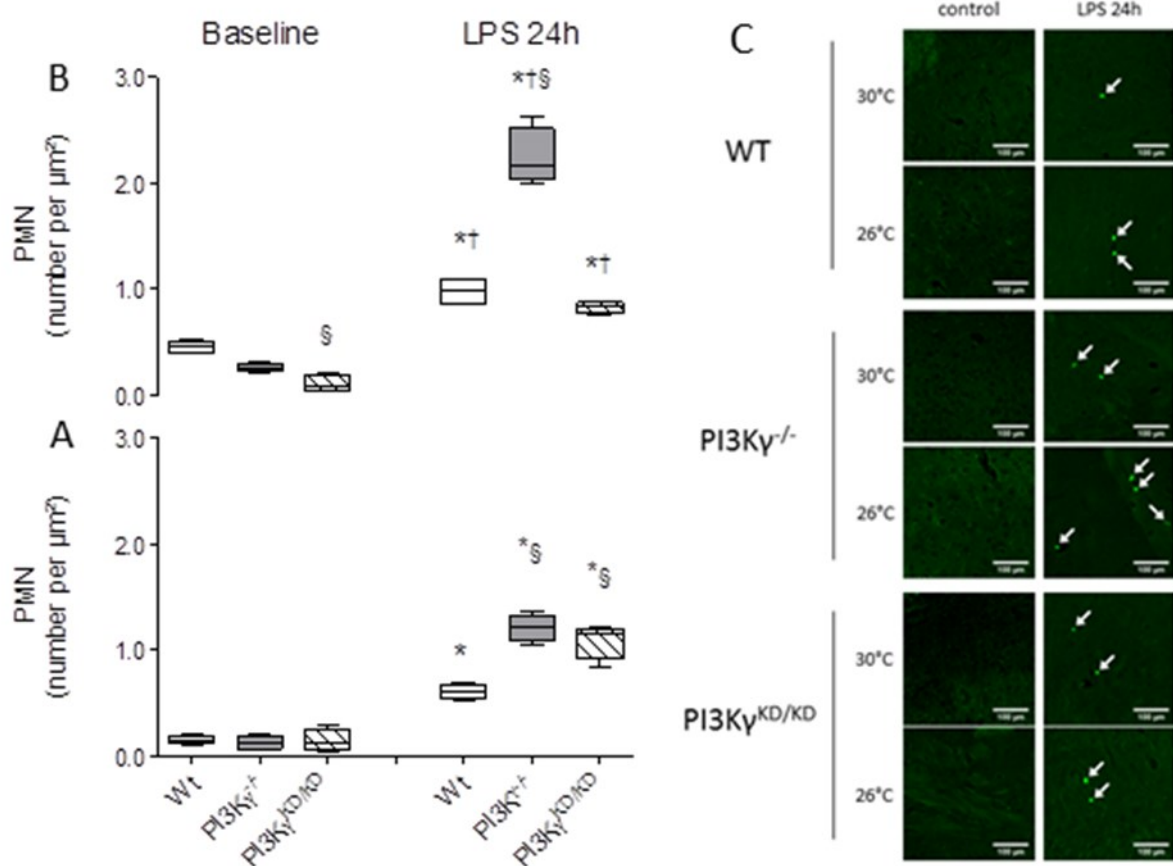

Figure 9. Influence of T_a on apoptosis.

Increased number of apoptotic cells in brains obtained from PI3K$\gamma^{-/-}$ and PI3K$\gamma^{KD/KD}$ mice kept under reduced T_a (B) compared to mice kept under neutral T_a (A) 24h after LPS administration. C: representative images. Values are presented as boxplots illustrating medians within boxes from first quartile to the third quartile and whiskers ranging from the 10th to the 90th percentiles (lower panel: neutral T_a, upper panel: reduced T_a, n=4 at each group and experimental state. * § † $p < 0.05$, * significant differences versus baseline at the same genotype and experimental state, § significant differences versus wild type mice kept under same T_a, † significant differences versus mice kept under neutral T_a at the same experimental state, two-way ANOVA, followed by Holm-Sidak test for post hoc multiple comparisons, each).

Regional comparison revealed that number of TUNEL-positive cells were markedly higher in the hippocampus, compared to cortex and thalamus, respectively (Tab. 8).

To assess a contribution of blood-born immune cells on pathogenesis of SIRS-induced SAE, the extent of invading PMN was gathered. Whereas under baseline conditions merely scattered PMN were encountered and neither T_a nor genotype-related effects has been ascertained, LPS-induced SIRS was accompanied by a marked increase of invading PMN into the brain tissue. We found a distinct T_a dependent effect in PI3Kγ-deficient mice because of an enhanced PMN homing into brain tissue in mice kept under reduced T_a (Fig. 10). However, a regional accentuation has not been verified (Tab. 8).

Figure 10. Influence of T_a on PMN invading.

Increased number of invading PMN in brains obtained from mice kept under reduced T_a (B) compared to mice kept under neutral T_a (A) 24h after LPS administration. This was more pronounced in brains obtained from PI3Kγ^{-/-} mice. C: representative images. Values are presented as boxplots illustrating medians within boxes from first quartile to the third quartile and whiskers ranging from the 10th to the 90th percentiles (lower panel: neutral T_a, upper panel: reduced T_a, n=4 at each group and experimental state. * [§] [†] $p < 0.05$, * significant differences versus baseline at the same genotype and experimental state, [§] significant differences versus wild type mice kept under same T_a, [†] significant differences versus mice kept under neutral T_a at the same experimental state, two-way ANOVA, followed by Holm–Sidak test for post hoc multiple comparisons, each).

### 3.3. Impact of T_a / T_{Inc} on microglial migration and phagocytosis

The ability to migrate toward different chemotactic stimuli including those released by brain injuries is one important property of microglial cells, which is essential for biological functions. Previous own studies revealed a dependency of lipid kinase-related PI3Kγ signaling on directed motility of microglial cells owing to inflammatory stimulation (Schneble et al. 2017b). Herein we addressed the question if PI3Kγ dependent migration of this cell type is a result of different ambient temperature or its *in vitro* surrogate, e.g. varied temperatures of incubation.

First, the *in vitro* cell motility was quantified toward migration to C5a added to bottom well of the transwell assay together with stimulation with LPS. C5a acts as inflammatory peptide resulting in stimulation of microglial migration toward this chemo attractant. As demonstrated in Figure 11, PI3Kγ-deficiency as well as targeted knockout of the lipid kinase activity of PI3Kγ caused a markedly reduced migratory capacity by about 50% compared with cells derived from wild type mice. A moderately reduced T_{Inc} provoked a further reduction in directed motility of primary microglial cell, whereas the PI3Kγ related migratory alteration remained preserved.

To assess the effect of PI3Kγ-deficiency on directed cell motility *in vivo*, a wound healing assay using focal stab-injury (Schneble et al. 2017a) was carried out (Fig. 11B). Whereas the basal number of microglial cells was similar in wild type, PI3Kγ deficient and -kinase dead brains (Tab. 9), migration of microglia in direction of the focal stab injury was clearly reduced in brains from PI3Kγ mutants as indicated by reduced microglial cell numbers in the outer regions of interest (Areas 2 and 3; 200 to 400 and 400 to 600 µm from the place of injury) of the injury site, which was markedly reduced in mice kept at reduced T_a. Taken together, data indicate an inhibitory role of reduced T_a for the directional migration/chemotaxis of microglia.

The role of modified ambient temperature for phagocytosis, as another essential function of microglia, was also analyzed. First, efficiency of phagocytosis was quantified by *in vitro* incubation of microglia with FITC-labeled Zymosan particles and subsequent counting of incorporated particles inside the microglial cells. PI3Kγ deficiency caused a distinct decrease of phagocytosis of microglial cells under normal T_{Inc} (Fig. 12A). Under reduced T_{Inc} quite similar effects has been ascertain. *In vivo* analysis of phagocytosis was performed by intracerebral administration of Zymosan particles. Counting the number of cells with phagocytosed particles revealed under neutral T_a a reduction of microglial phagocytic activity in brains de-

rived from PI3Kγ$^{-/-}$ mice. Reduced T_a caused a distinct inhibition of phagocytic activity which was more pronounced in PI3Kγ-deficient mice (Fig. 12B).
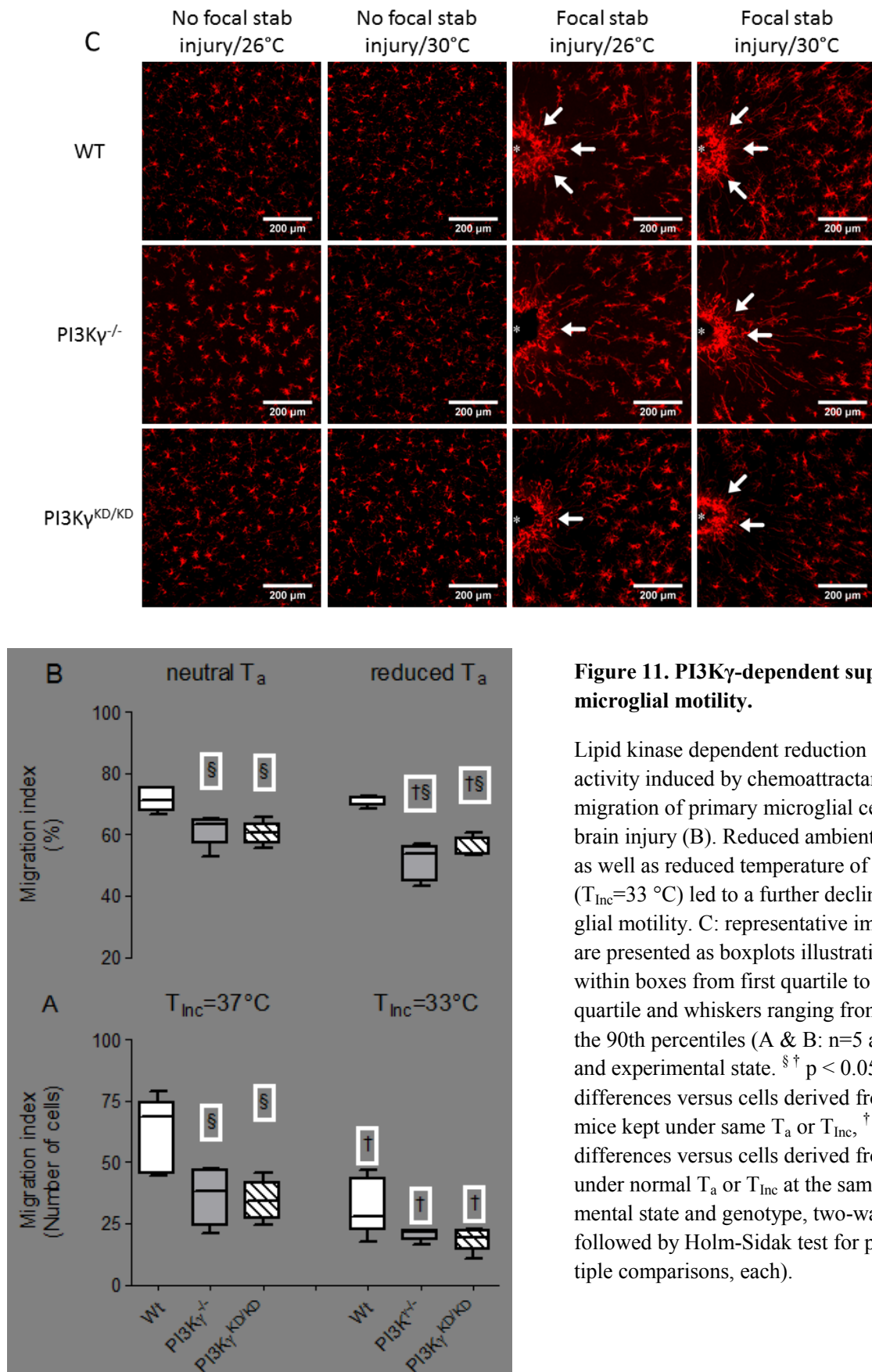
Figure 11. PI3Kγ-dependent suppression of microglial motility.

Lipid kinase dependent reduction of migratory activity induced by chemoattractant- stimulated migration of primary microglial cells (A) and brain injury (B). Reduced ambient temperature as well as reduced temperature of incubation (T_{Inc}=33 °C) led to a further decline of micro-glial motility. C: representative images. Values are presented as boxplots illustrating medians within boxes from first quartile to the third quartile and whiskers ranging from the 10th to the 90th percentiles (A & B: n=5 at each group and experimental state. $^{§ †}$ $p < 0.05$, § significant differences versus cells derived from wild type mice kept under same T_a or T_{Inc}, † significant differences versus cells derived from mice kept under normal T_a or T_{Inc} at the same experi-mental state and genotype, two-way ANOVA, followed by Holm-Sidak test for post hoc mul-tiple comparisons, each).

Table 8. Regional distribution of MMP-9 positive cells, TUNEL positive cells and invading polymorphonuclear leukocytes (PMN)

	Cortex		Hippocampus		Thalamus	
	Baseline	*24h-LPS*	*Baseline*	*24h-LPS*	*Baseline*	*24h-LPS*
MMP-9 positive cells						
Neutral T_a						
Wt	0.05 (0.05, 0.06)	0.34 (0.34, 0.37) *	0.14 (0.11, 0.14)	0.79 (0.69, 0.94) *	0.05 (0.04, 0.07)	0.42 (0.33, 0.49) *
PI3Kγ$^{-/-}$	0.07 (0.04, 0.1)	0.46 (0.44, 0.5) *	0.22 (0.11, 0.36)	0.72 (0.65, 1.01) *	0.08 (0.05, 0.11)	0.53 (0.37, 0.58) *
PI3Kγ$^{-KD/KD}$	0.07 (0.05, 0.15)	0.51 (0.45, 0.56) *	0.14 (0.11, 0.22)	1.44 (1.08, 1.8) *	0.05 (0, 0.11)	0.53 (0.37, 0.58) *
Reduced T_a						
Wt	0.07 (0.05, 0.11)	0.46 (0.42, 0.5) *	0.07 (0, 0.14)	0.72 (0.65, 0.79) *	0.03 (0, 0.07)	0.53 (0.53, 0.53) *
PI3Kγ$^{-/-}$	0.1 (0.1, 0.11)	0.73 (0.71, 0.75) *†§	0.22 (0.11, 0.29)	1.23 (0.76, 0.97) *†§	0.05 (0.04, 0.05)	0.32 (0.26, 0.28) *†§
PI3Kγ$^{-KD/KD}$	0.1 (0.07, 0.11)	0.61 (0.57, 0.66) *§	0.14 (0.11, 0.18)	0.87 (0.58, 1.3) *†§	0.08 (0.05, 0.12)	0.37 (0.3, 0.45) *§
TUNEL positive cells						
Neutral T_a						
Wt	0.27 (0.24, 0.29)	0.49 (0.44, 0.55)*	0.58 (0.54, 0.58)$^\$$	2.24 (2.13, 2.31)*$^\$$	0.05 (0.04, 0.07)	0.42 (0.33, 0.49) *
PI3Kγ$^{-/-}$	0.32 (0.28, 0.34)	0.64 (0.56, 0.68)*	1.01 (0.9, 1.08)$^\$$	1.37 (1.3, 1.59)*§$^\$$	0.08 (0.05, 0.11)	0.53 (0.37, 0.58) *
PI3Kγ$^{-KD/KD}$	0.29 (0.18, 0.42)	0.46 (0.4, 0.5)	0.5 (0.36, 0.61)$^\$$	1.01 (0.87, 1.19)*§$^\$$	0.05 (0, 0.11)	0.53 (0.37, 0.58) *
Reduced T_a						
Wt	0.29 (0.27, 0.33)	0.68 (0.66, 0.71)*	0.72 (0.43, 1.05)$^\$$	1.59 (1.55, 1.62)*†$^\$$	0.13 (0.11, 0.16)	0.29 (0.26, 0.32)*
PI3Kγ$^{-/-}$	0.29 (0.28, 0.33)	1 (0.93, 1.1)*†§	1.3 (1.23, 1.33)	2.81 (2.74, 3.03)*†§$^\$$	0.24 (0.2, 0.29)	0.66 (0.55, 0.68)*§
PI3Kγ$^{-KD/KD}$	0.29 (0.23, 0.34)	0.46 (0.4, 0.5)*§	0.65 (0.58, 0.76)$^\$$	1.95 (1.84, 2.09)*$^\$$	0.21 (0.18, 0.22)	0.42 (0.39, 0.42)*
Polymorphonuclear leukocytes						
Neutral T_a						
Wt	0.2 (0.2, 0.22)	0.83 (0.73, 0.86) *	0 (0, 0.07)	0.29 (0.29, 0.36) *	0.16 (0.11, 0.18)	0.58 (0.55, 0.6) *
PI3Kγ$^{-/-}$	0.1 (0.1, 0.15)	1.61 (1.34, 1.61) *	0 (0, 0.07)	1.15 (0.87, 1.23) *	0.05 (0.05, 0.11)	1 (0.97, 1.08) *
PI3Kγ$^{-KD/KD}$	0.24 (0.17, 0.27)	0.88 (0.78, 0.98) *	0.14 (0.07, 0.22)	1.59 (1.52, 1.8) *	0 (0, 0.13)	1.05 (0.89, 1.13) *
Reduced T_a						
Wt	0.44 (0.23, 0.46)	1.08 (0.95, 1.1) *	0.29 (0.22, 0.51)	1.44 (1.3, 1.52) *	0.37 (0.37, 0.39)	0.89 (0.87, 0.92) *
PI3Kγ$^{-/-}$	0.29 (0.27, 0.32)	2.64 (2.52, 2.71) *†§	0.14 (0.14, 0.22)	2.74 (2.53, 3.1) *†§	0.21 (0.18, 0.21)	1.68 (1.66, 1.92) *†§
PI3Kγ$^{-KD/KD}$	0.05 (0.05, 0.81)	0.78 (0.76, 0.27) *§	0 (0, 0.79)	0.72 (0.65, 0.22) *†§	0.05 (0.05, 0.97)	0.95 (0.87, 0.13) *§

(Values are given as medians as well as the first quartile and third quartile in parenthesis. n=4 at each group and experimental state. * † § $^\$$ $p < 0.05$, * significant differences versus baseline at the same genotype and experimental state, † significant differences versus mice kept under neutral T_a at the same experimental state, § significant differences versus wild type mice kept under same T_a, $^\$$ significant differences versus cortex & thalamus, two-way ANOVA, followed by Holm-Sidak test for post hoc multiple comparisons, each).

Table 9. Number of microglial cells in brain cortex

|	*Baseline*
Neutral T_a	
Wt	4483 (4447; 4554)
PI3Kγ$^{-/-}$	4132 (4099; 4371)
PI3Kγ$^{KD/KD}$	4536 (4362; 4653)
Reduced T_a	
Wt	4464 (4259; 4582)
PI3Kγ$^{-/-}$	4303 (4160; 4664)
PI3Kγ$^{KD/KD}$	4546 (4399; 4615)

(Values are given as medians as well as the first quartile and third quartile in parenthesis. n=7-8 at each group and experimental state, one-way ANOVA).

Therefore, reduced T_a enhanced the PI3Kγ dependent influence on microglial migration and phagocytosis.

## 3.4. Effects of T_{Inc} on cellular energetics of microglia

We evaluated the effects of normal and reduced T_{Inc} on the cellular energetics of microglia following 24 h of LPS treatment using the Seahorse XF96 Analyzer. Estimation of mitochondrial oxygen consumption rate (OCR) under baseline conditions revealed a small but significant OCR increase in PI3Kγ$^{-/-}$ cells when incubated under normal conditions, whereas microglia derived from PI3Kγ$^{KD/KD}$ mice exhibited a reduced respiration rate under normal and reduced T_{Inc} (Fig. 11). LPS stimulation provoked under normal incubation temperature a reduction of OCR in all genotypes under consideration, whereas just wild type cells showed the same behavior under reduced T_{Inc}. Furthermore, microglial cells derived from PI3Kγ$^{-/-}$ as well as PI3Kγ$^{KD/KD}$ mice, indicative for inhibition of the lipid kinase/AKT pathway, exhibited a reduced glycolytic activity (Fig. 13). Moreover, a reduced glycolytic activity occurred in microglial cells after LPS stimulation, when incubated at 33 °C.

These data indicate a rather minor impact of LPS stimulation on the cellular energetics of primary microglial cells.
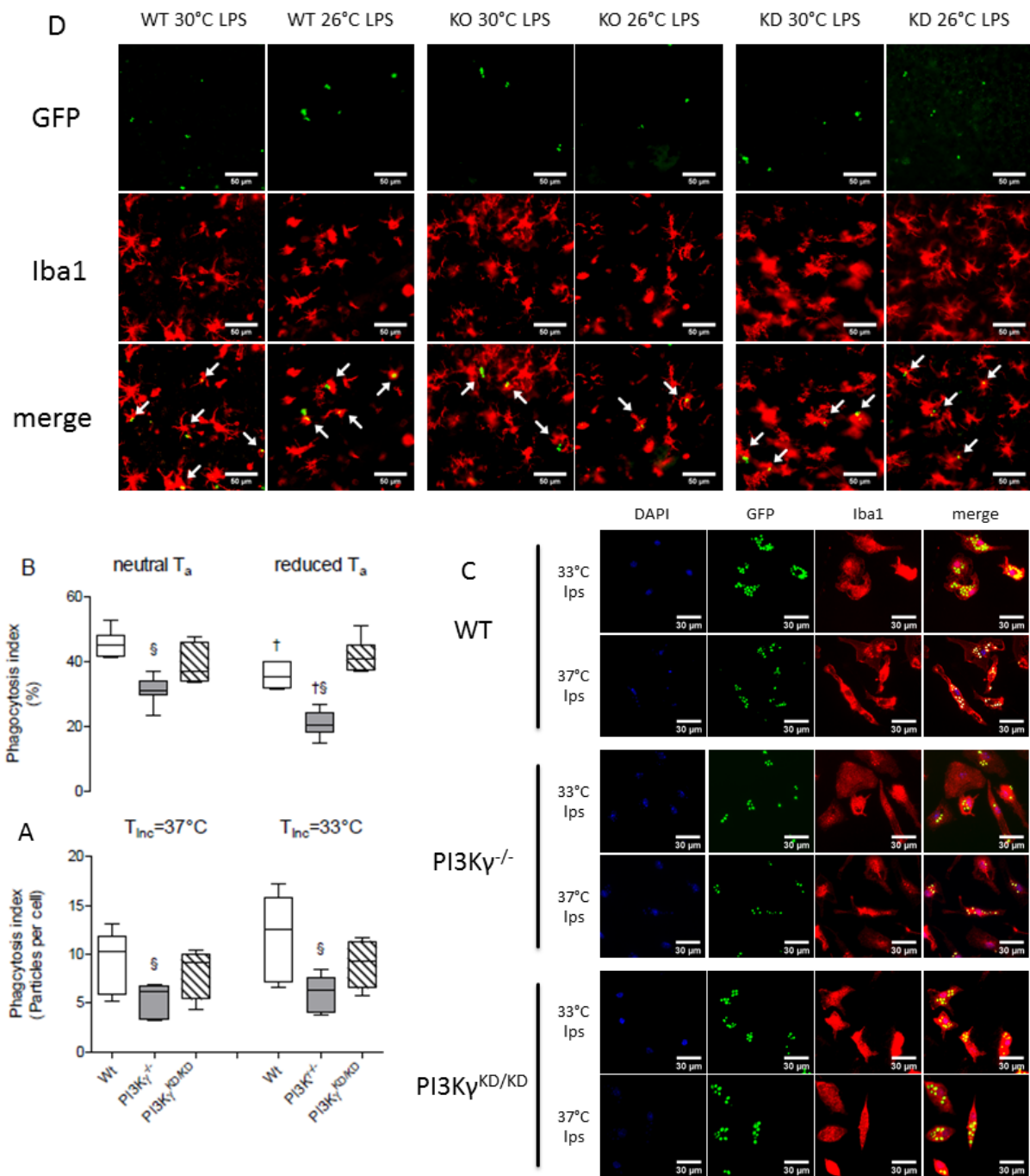
Figure 12. PI3Kγ-kinase activity independent suppression of phagocytic activity.

Under *in vivo* conditions, PI3Kγ lipid kinase independent reduction of phagocytosis induced a reduced phagocytic activity in mice kept under reduced T_a (B). C: Representative images from *in vitro* studies, D: representative images from *in vivo* studies. Values are presented as boxplots illustrating medians within boxes from first quartile to the third quartile and whiskers ranging from the 10th to the 90th percentiles (A: n=5, B: n=7 at each group and experimental state. [§ †] p < 0.05, [§] significant differences versus cells derived from wild type mice kept under same T_a or T_{Inc}, [†] significant differences versus cells derived from mice kept under normal T_a or T_{Inc} at the same experimental state and genotype, two-way ANOVA, followed by Holm–Sidak test for post hoc multiple comparisons, each).
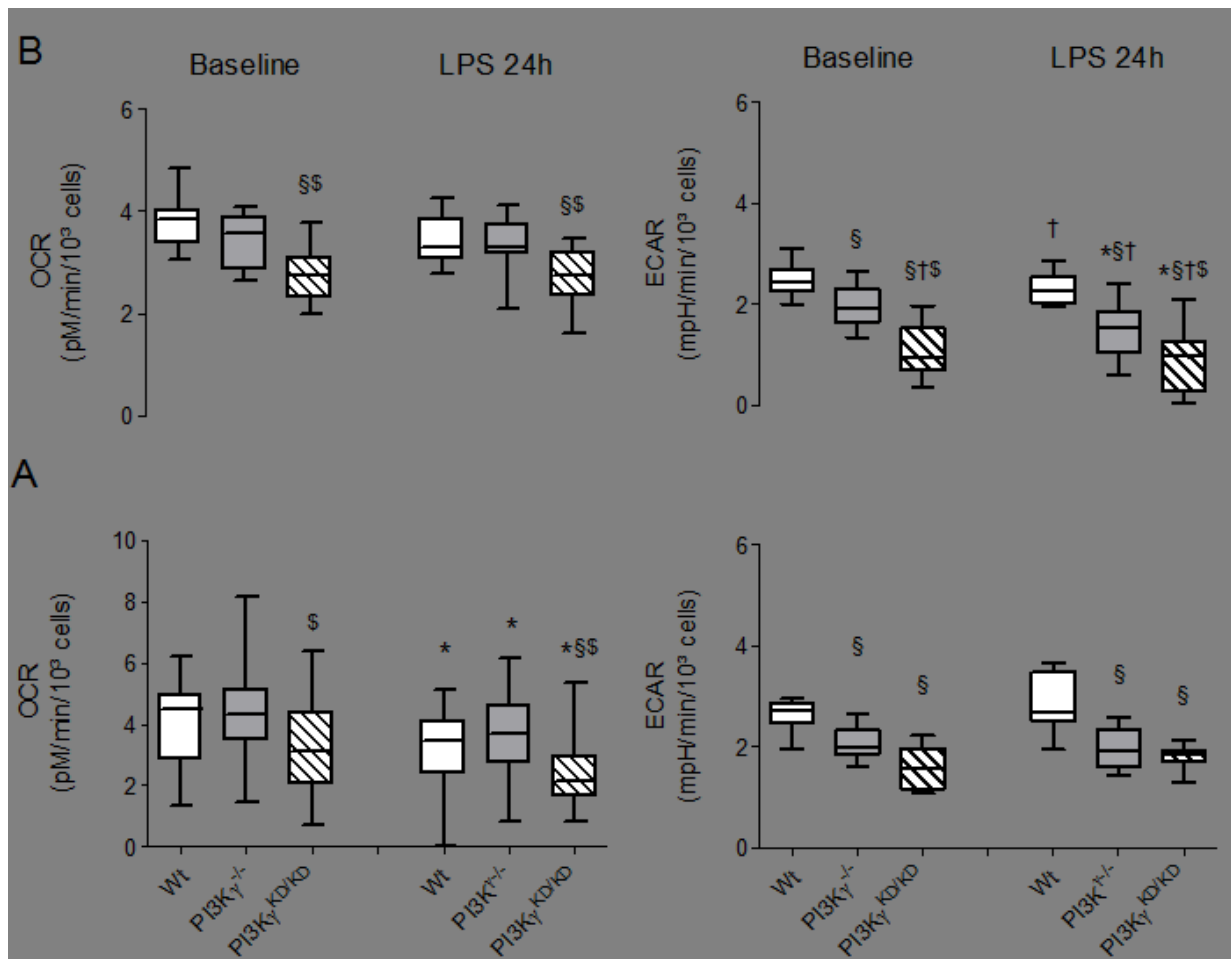
Figure 13. Effect of PI3Kγ on regulation of cellular energetics in primary microglia.

(A: T_{Inc}=37 °C, B T_{Inc}=33 °C; n=4 at each group and experimental state. OCR, basal oxygen consumption rate; ECAR, extracellular acidification rate). Values are presented as boxplots illustrating medians within boxes from first quartile to the third quartile and whiskers ranging from the 10th to the 90th percentiles. * [§] [†] [$] $p < 0.05$, [§] significant differences versus cells derived from wild type mice kept under same T_a, [†] significant differences versus cells derived from mice kept under normal T_a at the same experimental state and genotype, [$] compared to PI3Kγ^{-/-} at the same experimental state, two-way ANOVA, followed by Holm-Sidak test for post hoc multiple comparisons, each.

4. Discussion

4.1. Role of altered ambient temperature for SIRS pathogenesis

Our study identifies ambient temperature as a major impact factor for extent and clinical course of LPS-induced SIRS and concomitant BBB breakdown as a key event in the development of sepsis-induced brain injury. We studied LPS-induced SIRS at a T_a of 30 °C (within thermoneutral zone (Gordon 1991)) and at the upper edge of the recommended standard housing temperatures for laboratory mice, e.g. at 26 °C (NRC 2011). We show for the first time that a reduction of T_a of only 3-4 degrees below the lower critical T_a for mice (Gordon 2017) increases the severity of BBB injury as a consequence of LPS-induced SIRS. This was clearly associated with a temporary disturbance of thermoregulation as a fundamental homeostatic function of all mammals, because body core temperature was markedly reduced early after LPS-induced SIRS and hypothermia remained reduced throughout the observed period (Fig. 4). Occurrence of hypothermia as a result of sepsis/overwhelming systemic inflammation, however, characterizes a specific state of disturbed thermoregulation. Indeed, previous experimental and clinical studies clearly showed that severity of inflammation determines direction of displacement from normothermia, e.g. mild to moderate SIRS induced by low and medium dosages of LPS provoke fever, whereas severe/life-threatening SIRS induces hypothermia (Kushimoto et al. 2014; Romanovsky et al. 1996; Rudaya et al. 2005). The mechanisms regulating hypothermia are not fully understood, but cytokines such as tumor necrosis factor-alpha (TNFα), interleukins (ILs) and interferon-gamma have been shown to induce or modulate hypothermia (Leon 2004). The herein presented data suggest that TNFα may contribute to the hypothermic response because of a similar time course. However, other factors play apparently a more dominant role for the extent of hypothermia early after LPS-induced SIRS induction. Clearly, T_a determines depth of T_c reduction (Fig. 4). Therefore, hypothermic response appears to be a consequence of maladaptive thermoregulation leading to hypometabolism in order to avoid hypoxia (Corrigan et al. 2014). Even if this study was not designed to explore disturbed thermoregulation due to LPS-induced hypothermia, PI3Kγ-dependent differences in extent of sickness suggest that disturbance in behavioral thermoregulation may contribute to the manifestation of hypothermia. Small rodents like mice need an increased metabolic rate and periodic motor activity for appropriate heat production to maintain homeothermy because of its unfavourable surface area vs. mass relation (Cannon and Nedergaard 2011; Gordon 2017) and develop hypothermia when locomotor activity is diminished due to consequences of sickness induced by infection (Jhaveri et al. 2007). Furthermore, mice kept at reduced T_a developed an exacerbated and prolonged hypothermia although they exhibited a markedly

enhanced sympathetic tone. This might be related to a stronger impairment of thermoregulation with torpor-like traits induced by LPS-induced SIRS (Szentirmai and Krueger 2014) in addition to LPS-induced inhibition of brown adipose tissue thermogenesis (Okla et al. 2015).

The worsening consequences of sickness-induced hypothermia on SIRS-induced SAE and other sepsis related organ dysfunctions like septic cardiomyopathia (Ndongson-Dongmo et al. in revision), where we could show that moderate reduction of T_a led to a 40% enhanced mortality of mice undergoing LPS-induced SIRS, goes against potential beneficial consequences of treatment of critical ill patients with therapeutic hypothermia (i.e. in targeted temperature management as part of post-resuscitation care) or induced hypothermia (as used in deep hypothermic circulatory arrest (DHCA) for cardiovascular surgery) (Brown et al. 2012; Paal et al. 2016). This fundamental difference implies that the treatment-related forms of induced hypothermia are performed by drug-provoked elimination of thermoregulation with prevention of shivering and non-shivering heat production that means prevention of extra energy demand but use of organ protection by activation numerous signaling pathways preventing hypoxic cell loss (Polderman 2009; Yenari and Han 2012). Management of body temperature (T_c) in sepsis needs differentiating considerations. The frequently occurring fever enhances inflammation and energy demand (by 10% per extra 1 °C increase) but decrease bacterial and viral load. Therefore, normothermia (fever therapy) is regarded to be beneficial when bacterial load is controlled by antibiotics (Rice et al. 2005). Whilst the advantages of therapeutic control of fever in sepsis remain a controversial topic, there is now good evidence that external cooling or treatment with antipyretics to warrant normothermia were safe and effective in septic shock (Schortgen et al. 2012; Young et al. 2015). External cooling improves vascular tone, reduces oxygen consumption and improved short-term mortality. Treatment with antipyretics improves temporarily cardiovascular function. However, no difference in long-term mortality remained.

4.2. Appropriateness of research approaches to study septic encephalopathy

The complexity of sepsis makes the clinical study of sepsis and sepsis therapeutics difficult. Animal models have been developed in an effort to create reproducible systems for studying sepsis pathogenesis, preliminary testing of potential therapeutic agents and different components of this multi-faceted life-threatening disease. It is obvious that cerebral dysfunction in sepsis has been the focus of intense research activity.

Meanwhile it is recognized that for translational and therapy-targeted approaches appropriate infection models are indispensable (Buras et al. 2005; Dyson and Singer 2009; Rittirsch et al. 2007). Several well-standardized experimental approaches are described in order to perform an infection which develops a clinical picture associated with many prototypical features of sepsis culminating in sepsis associated multi-organ dysfunction. In principle, they can be divided into two categories: exogenous administration of a viable pathogen (such as bacteria); or alteration of the animal's endogenous protective barrier (inducing colonic permeability, allowing bacterial translocation) (Buras et al. 2005). However, despite its clinical relevance and widespread use in sepsis research, one of the major concerns of infection models is consistency (Rittirsch et al. 2009).

Consequently, for mechanistic approaches with time-critical requirements and attempt to verify definable components of sepsis, like the initial infection-induced SIRS, other elaborated approaches with high-grade standardized animal response are more appropriate. Therefore, we used the LPS model where a defined amount of endotoxin is given as systemic administration via instillation into the abdominal cavity leading to a uniform response of the host (i.e. mice mutants) with development of the full picture of infection-induced SIRS. Clearly, this approach is based on model of sepsis underlies the notion that it is the host response that causes the clinical features of sepsis and not the intact pathogen per se. Endotoxin is part of the outer membrane of the cell envelope of gram-negative bacteria. The term endotoxin is often used exchangeable with LPS, as LPS represents the main biologically active component of endotoxin. The i.v. infusion of LPS as well as its instillation into the abdominal cavity causes symptoms of severe infection, accompanied by similarities to pathophysiological responses in patients with sepsis, such as hematological alterations (Remick et al. 2000). Furthermore, LPS infusion induces an increase of proinflammatory cytokines in serum (Remick et al. 1990), another parallel to septic patients, whose elevated cytokine levels correlate with severity of the disease (Waage et al. 1987). However, the LPS experimental model and sepsis in humans differ in several key points, especially in profile and time course of cytokine release. Cytokine levels (TNF-α, IL-6, CXC chemokines) peaked much later and occurred at much lower levels in human patients with sepsis as well as infection models of sepsis when compared with effects of LPS infusion (Cavaillon et al. 2003; Gonnert et al. 2011; Remick et al. 2000). Nevertheless, when molecular mechanisms of organ-specific alterations during infection-induced SIRS are target of basic science studies - especially when SIRS is known to initiate early disturbances of organ function in sepsis - the LPS model in mouse mutants remain one of the most appropriate approaches in order to investigate organ-specific effect in intact animals. Of note, this approach enables cell-targeted approaches under comparable ex-

perimental conditions, e.g. cell-culture studies on primary cells (obtained from the same mouse mutants and stimulated with LPS in cell culture) for mechanistic investigations.

Therefore, we decide to use the LPS model to investigate the role of PI3Kγ in infection-induced SIRS in order to explore whether or not PI3Kγ is causally involved in pronounced BBB disturbance in virtue of SAE.

4.3. Role of PI3Kγ in SIRS-induced SAE

In a previous study, we have shown that the kinase-independent control of cAMP phosphodiesterase activity by PI3Kγ acts as a crucial mediator of microglial cell activation, MMP expression and subsequent BBB deterioration (Frister et al. 2014). The data obtained in the current study suggest that an aggravated BBB breakdown observed in mice kept at reduced T_a during LPS-induced SIRS results from an intensified LPS-induced proinflammatory microglial response with concomitantly pronounced upregulation of brain MMP expression and perivascular MMP-9 release leading to increased PMN invasion with altered microglial migration and phagocytosis. These processes appear to be widespread because there were similar findings in quite different brain regions under consideration. Enhanced plasma protein extravasation in brains obtained from PI3Kγ-deficient mice kept under reduced T_a suggests that the genotype-related differences in BBB breakdown appears to be related to microglial activation in response to systemic inflammation and concomitant brain tissue MMP upregulation. Compelling evidence suggests that early after SIRS manifestation, constitutive proteases are activated and begin the process of disassembling the extracellular matrix and opening the BBB (Candelario-Jalil et al. 2009; Rosenberg 2012). Immunohistological evaluation revealed that there is an increased number of Iba-1 positive cell which co-express MMP-9 in brains obtained from PI3Kγ-deficient mice kept under reduced T_a, which may play a crucial role to exacerbate BBB deterioration due to sequential activation by MMP-3 and subsequent attack the basal lamina and tight junction proteins (Candelario-Jalil et al. 2009; Gurney et al. 2006). Our previous results revealed that the enhanced MMP-9 activity is of microglial origin and provoked by a deficient suppressive control of cAMP-dependent signaling in PI3Kγ-deficient mice (Frister et al. 2014). MMP-9 is known to act as executing protease for degrading matrix substrates and interrupting cell-cell or cell-matrix homeostatic interactions, which may directly trigger anoikis-like neuronal cell death by interrupting cell-matrix survival signaling (Gu et al. 2002). The current findings of aggravated SIRS-induced BBB impairment associated with reduced T_a are clearly PI3Kγ-dependent and induce an enhanced invasion of blood born im-

mune cells and an increased rate of apoptosis when the suppressive effect of PI3Kγ on cAMP as a critical mediator of immune cell functions is absent (Figs. 9&10). Causal relations responsible for associated exacerbated brain injury cannot be drawn conclusively. Nevertheless, a reduced ability of directed motility and diminished phagocytic activity in brains obtained from PI3Kγ-deficient mice kept under reduced T_a suggest that these altered cell functions contribute to the phenotype of enhanced structural and functional cerebral disturbance leading to aggravate SAE-associated symptoms. Previous own findings identified the lipid kinase activity of PI3Kγ as an essential mediator of microglial migration (Schneble et al. 2017b). Furthermore, diminished microglial phagocytic activity appears to contribute to the enhanced proinflammatory brain response on LPS-induced SIRS in PI3Kγ-deficient mice kept under reduced T_a because microglial phagocytosis represents a key factor for limitation of excessive proinflammatory activation by clearance of dying cells and debris in injured brain tissue (Kettenmann et al. 2011; Neumann et al. 2009; Schmidt et al. 2016). Therefore, our findings support previous reports on inhibition of microglial phagocytosis caused by abnormal high cAMP levels though PKA and Epac (Makranz et al. 2006).

Till now, just few studies have addressed the pathological implications of altered energy metabolism including mitochondrial dysfunction in glial cells and its consequences in neurological disorders (Rose et al. 2017). A proinflammatory phenotype of microglia was recently reported to be paralleled by a metabolic switch from mitochondrial oxygen consumption rate to glycolysis that enhances carbon flux to the pentose phosphate pathway (Gimeno-Bayon et al. 2014; Orihuela et al. 2016; Voloboueva et al. 2013). We found just a minor reduction of oxygen consumption rate at neutral T_a. Reasons remained uncertain keeping in mind that the previous reported data were obtained from immortalized microglial cell lines whereas we studied primary microglial cells.

5. Conclusion

Results clearly underline the importance of ambient temperature as a frequently neglected environmental condition in translational work of inflammatory/infectious research. The major significance of the of herein presented data is that - despite preadaptation on discrete ambient climate conditions - the modest variation of an easily controllable parameter, i.e., ambient temperature led to a serious impact in the course of SIRS-associated SAE. Furthermore, our data disclose the signaling protein PI3Kγ as a critical mediator of key microglial cell functions involved in LPS-induced BBB injury and accompanied neuroinflammation. PI3Kγ serves a protective role in that it suppresses MMP release, maintains microglial motility and reinforces phagocytosis leading to improved brain tissue integrity.

Therefore, PI3Kγ seems a mediator of certain immune functions (phagocytosis, migration, MMP production), which are induced by infections and which are accompanied by environmental factors like T_a with potential impact for aggravating inflammatory events.

References

Abreu-Vieira G, Xiao C, Gavrilova O, Reitman ML. 2015. Integration of body temperature into the analysis of energy expenditure in the mouse. Mol Metab 4:461-70.

Alessi DR, Andjelkovic M, Caudwell B, Cron P, Morrice N, Cohen P, Hemmings BA. 1996. Mechanism of activation of protein kinase B by insulin and IGF-1. EMBO J 15:6541-51.

Angus DC, van der Poll T. 2013. Severe sepsis and septic shock. N Engl J Med 369:840-51.

Banks WA. 2005. Blood-brain barrier transport of cytokines: a mechanism for neuropathology. Curr Pharm Des 11:973-84.

Banks WA, Erickson MA. 2010. The blood-brain barrier and immune function and dysfunction. Neurobiol Dis 37:26-32.

Banks WA, Robinson SM. 2010. Minimal penetration of lipopolysaccharide across the murine blood-brain barrier. Brain Behav Immun 24:102-9.

Bauer M, Coldewey SM, Leitner M, Loffler B, Weis S, Wetzker R. 2018. Deterioration of Organ Function As a Hallmark in Sepsis: The Cellular Perspective. Front Immunol 9:1460.

Bone RC, Sibbald WJ, Sprung CL. 1992. The ACCP-SCCM consensus conference on sepsis and organ failure. Chest 101:1481-3.

Brightman MW, Reese TS. 1969. Junctions between intimately apposed cell membranes in the vertebrate brain. J Cell Biol 40:648-77.

Brodhun M, Fritz H, Walter B, Antonow-Schlorke I, Reinhart K, Zwiener U, Bauer R, Patt S. 2001. Immunomorphological sequelae of severe brain injury induced by fluid-percussion in juvenile pigs--effects of mild hypothermia. Acta Neuropathol 101:424-34.

Brown DJ, Brugger H, Boyd J, Paal P. 2012. Accidental hypothermia. N Engl J Med 367:1930-8.

Buras JA, Holzmann B, Sitkovsky M. 2005. Animal models of sepsis: setting the stage. Nat Rev Drug Discov 4:854-65.

Burke JE, Williams RL. 2013. Dynamic steps in receptor tyrosine kinase mediated activation of class IA phosphoinositide 3-kinases (PI3K) captured by H/D exchange (HDX-MS). Adv Biol Regul 53:97-110.

Candelario-Jalil E, Yang Y, Rosenberg GA. 2009. Diverse roles of matrix metalloproteinases and tissue inhibitors of metalloproteinases in neuroinflammation and cerebral ischemia. Neuroscience 158:983-94.

Cannon B, Nedergaard J. 2011. Nonshivering thermogenesis and its adequate measurement in metabolic studies. J Exp Biol 214:242-53.

Cantley LC. 2002. The phosphoinositide 3-kinase pathway. Science 296:1655-7.

Cavaillon JM, Adib-Conquy M, Fitting C, Adrie C, Payen D. 2003. Cytokine cascade in sepsis. Scand J Infect Dis 35:535-44.

Cerra FB. 1985. The systemic septic response: multiple systems organ failure. Crit Care Clin 1:591-607.

Charkoudian N, Wallin BG. 2014. Sympathetic neural activity to the cardiovascular system: integrator of systemic physiology and interindividual characteristics. Compr Physiol 4:825-50.

Clemmer TP, Fisher CJ, Jr., Bone RC, Slotman GJ, Metz CA, Thomas FO. 1992. Hypothermia in the sepsis syndrome and clinical outcome. The Methylprednisolone Severe Sepsis Study Group. Crit Care Med 20:1395-401.

Comim CM, Vilela MC, Constantino LS, Petronilho F, Vuolo F, Lacerda-Queiroz N, Rodrigues DH, da Rocha JL, Teixeira AL, Quevedo J and others. 2011. Traffic of leukocytes and cytokine up-regulation in the central nervous system in sepsis. Intensive Care Med 37:711-8.

Corrigan JJ, Fonseca MT, Flatow EA, Lewis K, Steiner AA. 2014. Hypometabolism and hypothermia in the rat model of endotoxic shock: independence of circulatory hypoxia. J Physiol 592:3901-16.

Costa C, Martin-Conte EL, Hirsch E. 2011. Phosphoinositide 3-kinase p110gamma in immunity. IUBMB Life 63:707-13.

Cumming J, Purdue GF, Hunt JL, O'Keefe GE. 2001. Objective estimates of the incidence and consequences of multiple organ dysfunction and sepsis after burn trauma. J Trauma 50:510-5.

Dantzer R, O'Connor JC, Freund GG, Johnson RW, Kelley KW. 2008. From inflammation to sickness and depression: when the immune system subjugates the brain. Nat Rev Neurosci 9:46-56.

Danzl DF, Pozos RS. 1994. Accidental hypothermia. The New England journal of medicine 331:1756-60.

Dellinger RP, Levy MM, Rhodes A, Annane D, Gerlach H, Opal SM, Sevransky JE, Sprung CL, Douglas IS, Jaeschke R and others. 2013. Surviving Sepsis Campaign: international guidelines for management of severe sepsis and septic shock, 2012. Intensive Care Med 39:165-228.

Dyson A, Singer M. 2009. Animal models of sepsis: why does preclinical efficacy fail to translate to the clinical setting? Crit Care Med 37:S30-7.

Ebersoldt M, Sharshar T, Annane D. 2007. Sepsis-associated delirium. Intensive Care Med 33:941-50.

Engelman JA, Luo J, Cantley LC. 2006. The evolution of phosphatidylinositol 3-kinases as regulators of growth and metabolism. Nat Rev Genet 7:606-19.

Erickson MA, Banks WA. 2018. Neuroimmune Axes of the Blood-Brain Barriers and Blood-Brain Interfaces: Bases for Physiological Regulation, Disease States, and Pharmacological Interventions. Pharmacol Rev 70:278-314.

Esen F, Senturk E, Ozcan PE, Ahishali B, Arican N, Orhan N, Ekizoglu O, Kucuk M, Kaya M. 2012. Intravenous immunoglobulins prevent the breakdown of the blood-brain barrier in experimentally induced sepsis. Crit Care Med 40:1214-20.

Eyolfson DA, Tikuisis P, Xu X, Weseen G, Giesbrecht GG. 2001. Measurement and prediction of peak shivering intensity in humans. Eur J Appl Physiol 84:100-6.

Feinstein DL, Heneka MT, Gavrilyuk V, Dello Russo C, Weinberg G, Galea E. 2002. Noradrenergic regulation of inflammatory gene expression in brain. Neurochem Int 41:357-65.

Franco I, Gulluni F, Campa CC, Costa C, Margaria JP, Ciraolo E, Martini M, Monteyne D, De Luca E, Germena G and others. 2014. PI3K class II alpha controls spatially restricted endosomal PtdIns3P and Rab11 activation to promote primary cilium function. Dev Cell 28:647-58.

Frister A, Schmidt C, Schneble N, Brodhun M, Gonnert FA, Bauer M, Hirsch E, Muller JP, Wetzker R, Bauer R. 2014. Phosphoinositide 3-kinase gamma affects LPS-induced disturbance of blood-brain barrier via lipid kinase-independent control of cAMP in microglial cells. Neuromolecular Med 16:704-13.

Funk DJ, Parrillo JE, Kumar A. 2009. Sepsis and septic shock: a history. Crit Care Clin 25:83-101, viii.

Gerencser AA, Neilson A, Choi SW, Edman U, Yadava N, Oh RJ, Ferrick DA, Nicholls DG, Brand MD. 2009. Quantitative microplate-based respirometry with correction for oxygen diffusion. Anal Chem 81:6868-78.

Gimeno-Bayon J, Lopez-Lopez A, Rodriguez MJ, Mahy N. 2014. Glucose pathways adaptation supports acquisition of activated microglia phenotype. J Neurosci Res 92:723-31.

Gofton TE, Young GB. 2012. Sepsis-associated encephalopathy. Nat Rev Neurol 8:557-66.

Gonnert FA, Recknagel P, Seidel M, Jbeily N, Dahlke K, Bockmeyer CL, Winning J, Losche W, Claus RA, Bauer M. 2011. Characteristics of clinical sepsis reflected in a reliable and reproducible rodent sepsis model. J Surg Res 170:e123-34.

Gordon CJ. 1991. Toxic-induced hypothermia and hypometabolism: do they increase uncertainty in the extrapolation of toxicological data from experimental animals to humans? Neurosci Biobehav Rev 15:95-8.

Gordon CJ. 2009. Quantifying the instability of core temperature in rodents. J Therm Biol 34:213–219.

Gordon CJ. 2012. Thermal physiology of laboratory mice: defining thermoneutrality J Therm Biol 37:654-685.

Gordon CJ. 2017. The mouse thermoregulatory system: Its impact on translating biomedical data to humans. Physiol Behav 179:55-66.

Gordon CJ, Becker P, Ali JS. 1998. Behavioral thermoregulatory responses of single- and group-housed mice. Physiol Behav 65:255-62.

Gordon CJ, Puckett ET, Repasky ES, Johnstone AF. 2017. A Device that Allows Rodents to Behaviorally Thermoregulate when Housed in Vivariums. J Am Assoc Lab Anim Sci 56:173-176.

Greter M, Lelios I, Croxford AL. 2015. Microglia Versus Myeloid Cell Nomenclature during Brain Inflammation. Front Immunol 6:249.

Gu Z, Kaul M, Yan B, Kridel SJ, Cui J, Strongin A, Smith JW, Liddington RC, Lipton SA. 2002. S-nitrosylation of matrix metalloproteinases: signaling pathway to neuronal cell death. Science 297:1186-90.

Gurney KJ, Estrada EY, Rosenberg GA. 2006. Blood-brain barrier disruption by stromelysin-1 facilitates neutrophil infiltration in neuroinflammation. Neurobiol Dis 23:87-96.

Gustot T. 2011. Multiple organ failure in sepsis: prognosis and role of systemic inflammatory response. Curr Opin Crit Care 17:153-9.

Gyoneva S, Traynelis SF. 2013. Norepinephrine modulates the motility of resting and activated microglia via different adrenergic receptors. J Biol Chem 288:15291-302.

Hanisch UK, Kettenmann H. 2007. Microglia: active sensor and versatile effector cells in the normal and pathologic brain. Nat Neurosci 10:1387-94.

Heublein S, Hartmann M, Hagel S, Hutagalung R, Brunkhorst FM. 2013. Epidemiology of sepsis in German hospitals derived from administrative databases. Infection 41:S71.

Hirsch E, Braccini L, Ciraolo E, Morello F, Perino A. 2009. Twice upon a time: PI3K's secret double life exposed. Trends Biochem Sci 34:244-8.

Hirsch E, Costa C, Ciraolo E. 2007. Phosphoinositide 3-kinases as a common platform for multi-hormone signaling. J Endocrinol 194:243-56.

Hirsch E, Katanaev VL, Garlanda C, Azzolino O, Pirola L, Silengo L, Sozzani S, Mantovani A, Altruda F, Wymann MP. 2000. Central role for G protein-coupled phosphoinositide 3-kinase gamma in inflammation. Science 287:1049-53.

Jensen TL, Kiersgaard MK, Sorensen DB, Mikkelsen LF. 2013. Fasting of mice: a review. Lab Anim 47:225-40.

Jhaveri KA, Trammell RA, Toth LA. 2007. Effect of environmental temperature on sleep, locomotor activity, core body temperature and immune responses of C57BL/6J mice. Brain Behav Immun 21:975-87.

Jin R, Yu S, Song Z, Quillin JW, Deasis DP, Penninger JM, Nanda A, Granger DN, Li G. 2010. Phosphoinositide 3-kinase-gamma expression is upregulated in brain microglia and contributes to ischemia-induced microglial activation in acute experimental stroke. Biochem Biophys Res Commun 399:458-64.

Johnson Z, Power CA, Weiss C, Rintelen F, Ji H, Ruckle T, Camps M, Wells TN, Schwarz MK, Proudfoot AE and others. 2004. Chemokine inhibition--why, when, where, which and how? Biochem Soc Trans 32:366-77.

Kettenmann H, Hanisch UK, Noda M, Verkhratsky A. 2011. Physiology of microglia. Physiol Rev 91:461-553.

Kotas ME, Medzhitov R. 2015. Homeostasis, inflammation, and disease susceptibility. Cell 160:816-827.

Kushimoto S, Yamanouchi S, Endo T, Sato T, Nomura R, Fujita M, Kudo D, Omura T, Miyagawa N, Sato T. 2014. Body temperature abnormalities in non-neurological critically ill patients: a review of the literature. J Intensive Care 2:14.

Laflamme N, Rivest S. 2001. Toll-like receptor 4: the missing link of the cerebral innate immune response triggered by circulating gram-negative bacterial cell wall components. FASEB J 15:155-163.

Laurent PA, Severin S, Gratacap MP, Payrastre B. 2014. Class I PI 3-kinases signaling in platelet activation and thrombosis: PDK1/Akt/GSK3 axis and impact of PTEN and SHIP1. Adv Biol Regul 54:162-74.

Lawson LJ, Perry VH, Dri P, Gordon S. 1990. Heterogeneity in the distribution and morphology of microglia in the normal adult mouse brain. Neuroscience 39:151-70.

Leevers SJ, Vanhaesebroeck B, Waterfield MD. 1999. Signalling through phosphoinositide 3-kinases: the lipids take centre stage. Curr Opin Cell Biol 11:219-25.

Leon LR. 2004. Hypothermia in systemic inflammation: role of cytokines. Front Biosci 9:1877-88.

Leon LR, Gordon CJ, Helwig BG, Rufolo DM, Blaha MD. 2010. Thermoregulatory, behavioral, and metabolic responses to heatstroke in a conscious mouse model. Am J Physiol Regul Integr Comp Physiol 299:R241-8.

Levy MM, Fink MP, Marshall JC, Abraham E, Angus D, Cook D, Cohen J, Opal SM, Vincent JL, Ramsay G and others. 2003. 2001 SCCM/ESICM/ACCP/ATS/SIS International Sepsis Definitions Conference. Crit Care Med 31:1250-6.

Livak KJ, Schmittgen TD. 2001. Analysis of relative gene expression data using real-time quantitative PCR and the 2(-Delta Delta C(T)) Method. Methods 25:402-8.

Lopez-Ilasaca M, Crespo P, Pellici PG, Gutkind JS, Wetzker R. 1997. Linkage of G protein-coupled receptors to the MAPK signaling pathway through PI 3-kinase gamma. Science 275:394-7.

Lossinsky AS, Shivers RR. 2004. Structural pathways for macromolecular and cellular transport across the blood-brain barrier during inflammatory conditions. Review. Histol Histopathol 19:535-64.

Majno G. 1991. The ancient riddle of sigma eta psi iota sigma (sepsis). J Infect Dis 163:937-45.

Makranz C, Cohen G, Reichert F, Kodama T, Rotshenker S. 2006. cAMP cascade (PKA, Epac, adenylyl cyclase, Gi, and phosphodiesterases) regulates myelin phagocytosis mediated by complement receptor-3 and scavenger receptor-AI/II in microglia and macrophages. Glia 53:441-8.

Mayhan WG. 1998. Effect of lipopolysaccharide on the permeability and reactivity of the cerebral microcirculation: role of inducible nitric oxide synthase. Brain Res 792:353-7.

Mazeraud A, Pascal Q, Verdonk F, Heming N, Chretien F, Sharshar T. 2016. Neuroanatomy and Physiology of Brain Dysfunction in Sepsis. Clin Chest Med 37:333-45.

Medzhitov R, Schneider DS, Soares MP. 2012. Disease tolerance as a defense strategy. Science 335:936-41.

Molnar L, Fulesdi B, Nemeth N, Molnar C. 2018. Sepsis-associated encephalopathy: A review of literature. Neurol India 66:352-361.

Nag S, Kapadia A, Stewart DJ. 2011. Review: molecular pathogenesis of blood-brain barrier breakdown in acute brain injury. Neuropathol Appl Neurobiol 37:3-23.

Nagyoszi P, Nyul-Toth A, Fazakas C, Wilhelm I, Kozma M, Molnar J, Hasko J, Krizbai IA. 2015. Regulation of NOD-like receptors and inflammasome activation in cerebral endothelial cells. J Neurochem 135:551-64.

Nagyoszi P, Wilhelm I, Farkas AE, Fazakas C, Dung NT, Hasko J, Krizbai IA. 2010. Expression and regulation of toll-like receptors in cerebral endothelial cells. Neurochem Int 57:556-64.

Nakamura K. 2011. Central circuitries for body temperature regulation and fever. Am J Physiol Regul Integr Comp Physiol 301:R1207-28.

Ndongson-Dongmo B, Heller R, Hoyer D, Brodhun M, Bauer M, Winning J, Hirsch E, Wetzker R, Schlattmann P, Bauer R. 2015. Phosphoinositide 3-kinase gamma controls inflammation-induced myocardial depression via sequential cAMP and iNOS signalling. Cardiovasc Res 108:243-53.

Ndongson-Dongmo B, Lang G-P, Mece O, Hechaichi N, Lajqi T, Hoyer D, Brodhun M, Heller R, Wetzker R, Levy FO and others. in revision. Reduced ambient temperature exacerbates SIRS-induced cardiac autonomic dysregulation and myocardial dysfunction in mice.

Neumann H, Kotter MR, Franklin RJ. 2009. Debris clearance by microglia: an essential link between degeneration and regeneration. Brain 132:288-95.

Nienaber JJ, Tachibana H, Naga Prasad SV, Esposito G, Wu D, Mao L, Rockman HA. 2003. Inhibition of receptor-localized PI3K preserves cardiac beta-adrenergic receptor function and ameliorates pressure overload heart failure. J Clin Invest 112:1067-79.

Nimmerjahn A, Kirchhoff F, Helmchen F. 2005. Resting microglial cells are highly dynamic surveillants of brain parenchyma in vivo. Science 308:1314-8.

NRC. 2011. Guide for the Care and Use of Laboratory Animals. Council of the National Academy of Science. Washington,DC: The National Academy Press.

O'Brown NM, Pfau SJ, Gu C. 2018. Bridging barriers: a comparative look at the blood-brain barrier across organisms. Genes Dev 32:466-478.

Odorizzi G, Babst M, Emr SD. 2000. Phosphoinositide signaling and the regulation of membrane trafficking in yeast. Trends Biochem Sci 25:229-35.

Okla M, Wang W, Kang I, Pashaj A, Carr T, Chung S. 2015. Activation of Toll-like receptor 4 (TLR4) attenuates adaptive thermogenesis via endoplasmic reticulum stress. J Biol Chem 290:26476-90.

Orihuela R, McPherson CA, Harry GJ. 2016. Microglial M1/M2 polarization and metabolic states. Br J Pharmacol 173:649-65.

Overton JM, Williams TD. 2004. Behavioral and physiologic responses to caloric restriction in mice. Physiol Behav 81:749-54.

Paal P, Gordon L, Strapazzon G, Brodmann Maeder M, Putzer G, Walpoth B, Wanscher M, Brown D, Holzer M, Broessner G and others. 2016. Accidental hypothermia-an update : The content of this review is endorsed by the International Commission for Mountain Emergency Medicine (ICAR MEDCOM). Scand J Trauma Resusc Emerg Med 24:111.

Papadopoulos MC, Davies DC, Moss RF, Tighe D, Bennett ED. 2000. Pathophysiology of septic encephalopathy: a review. Crit Care Med 28:3019-24.

Patrucco E, Notte A, Barberis L, Selvetella G, Maffei A, Brancaccio M, Marengo S, Russo G, Azzolino O, Rybalkin SD and others. 2004. PI3Kgamma modulates the cardiac response to chronic pressure overload by distinct kinase-dependent and -independent effects. Cell 118:375-87.

Paxinos G, Franklin KBJ. 2001. The Mouse Brain in Stereotaxic Coordinates. San Diego: Academic Press.

Polderman KH. 2009. Mechanisms of action, physiological effects, and complications of hypothermia. Crit Care Med 37:S186-202.

Reese TS, Karnovsky MJ. 1967. Fine structural localization of a blood-brain barrier to exogenous peroxidase. J Cell Biol 34:207-17.

Remick DG, Newcomb DE, Bolgos GL, Call DR. 2000. Comparison of the mortality and inflammatory response of two models of sepsis: lipopolysaccharide vs. cecal ligation and puncture. Shock 13:110-6.

Remick DG, Strieter RM, Eskandari MK, Nguyen DT, Genord MA, Raiford CL, Kunkel SL. 1990. Role of tumor necrosis factor-alpha in lipopolysaccharide-induced pathologic alterations. Am J Pathol 136:49-60.

Rice P, Martin E, He JR, Frank M, DeTolla L, Hester L, O'Neill T, Manka C, Benjamin I, Nagarsekar A and others. 2005. Febrile-range hyperthermia augments neutrophil accumulation and enhances lung injury in experimental gram-negative bacterial pneumonia. J Immunol 174:3676-85.

Rittirsch D, Hoesel LM, Ward PA. 2007. The disconnect between animal models of sepsis and human sepsis. J Leukoc Biol 81:137-43.

Rittirsch D, Huber-Lang MS, Flierl MA, Ward PA. 2009. Immunodesign of experimental sepsis by cecal ligation and puncture. Nat Protoc 4:31-6.

Romanovsky AA, Shido O, Sakurada S, Sugimoto N, Nagasaka T. 1996. Endotoxin shock: thermoregulatory mechanisms. Am J Physiol 270:R693-703.

Rose J, Brian C, Woods J, Pappa A, Panayiotidis MI, Powers R, Franco R. 2017. Mitochondrial dysfunction in glial cells: Implications for neuronal homeostasis and survival. Toxicology 391:109-115.

Rosenberg GA. 2012. Neurological diseases in relation to the blood-brain barrier. J Cereb Blood Flow Metab 32:1139-51.

Ruckle T, Schwarz MK, Rommel C. 2006. PI3Kgamma inhibition: towards an 'aspirin of the 21st century'? Nat Rev Drug Discov 5:903-18.

Rudaya AY, Steiner AA, Robbins JR, Dragic AS, Romanovsky AA. 2005. Thermoregulatory responses to lipopolysaccharide in the mouse: dependence on the dose and ambient temperature. Am J Physiol Regul Integr Comp Physiol 289:R1244-52.

Rudiger A, Fischler M, Harpes P, Gasser S, Hornemann T, von Eckardstein A, Maggiorini M. 2008. In critically ill patients, B-type natriuretic peptide (BNP) and N-terminal pro-BNP levels correlate with C-reactive protein values and leukocyte counts. Int J Cardiol 126:28-31.

Schmidt C, Frahm C, Schneble N, Muller JP, Brodhun M, Franco I, Witte OW, Hirsch E, Wetzker R, Bauer R. 2016. Phosphoinositide 3-Kinase gamma Restrains Neurotoxic Effects of Microglia After Focal Brain Ischemia. Mol Neurobiol 53:5468-79.

Schmidt C, Schneble N, Muller JP, Bauer R, Perino A, Marone R, Rybalkin SD, Wymann MP, Hirsch E, Wetzker R. 2013. Phosphoinositide 3-kinase gamma mediates microglial phagocytosis via lipid kinase-independent control of cAMP. Neuroscience 233:44-53.

Schneble N, Muller J, Kliche S, Bauer R, Wetzker R, Bohmer FD, Wang ZQ, Muller JP. 2017a. The protein-tyrosine phosphatase DEP-1 promotes migration and phagocytic activity of microglial cells in part through negative regulation of fyn tyrosine kinase. Glia 65:416-428.

Schneble N, Schmidt C, Bauer R, Muller JP, Monajembashi S, Wetzker R. 2017b. Phosphoinositide 3-kinase gamma ties chemoattractant- and adrenergic control of microglial motility. Mol Cell Neurosci 78:1-8.

Schortgen F. 2012. Fever in sepsis. Minerva Anestesiol 78:1254-64.

Schortgen F, Clabault K, Katsahian S, Devaquet J, Mercat A, Deye N, Dellamonica J, Bouadma L, Cook F, Beji O and others. 2012. Fever control using external cooling in septic shock: a randomized controlled trial. Am J Respir Crit Care Med 185:1088-95.

Schreiber R, Diwoky C, Schoiswohl G, Feiler U, Wongsiriroj N, Abdellatif M, Kolb D, Hoeks J, Kershaw EE, Sedej S and others. 2017. Cold-Induced Thermogenesis Depends on ATGL-Mediated Lipolysis in Cardiac Muscle, but Not Brown Adipose Tissue. Cell Metab 26:753-763 e7.

Semmler A, Widmann CN, Okulla T, Urbach H, Kaiser M, Widman G, Mormann F, Weide J, Fliessbach K, Hoeft A and others. 2013. Persistent cognitive impairment, hippocampal atrophy and EEG changes in sepsis survivors. J Neurol Neurosurg Psychiatry 84:62-9.

Seo JW, Kim JH, Kim JH, Seo M, Han HS, Park J, Suk K. 2012. Time-dependent effects of hypothermia on microglial activation and migration. J Neuroinflammation 9:164.

Sessler DI. 2016. Perioperative thermoregulation and heat balance. Lancet 387:2655-2664.

Seymour CW, Liu VX, Iwashyna TJ, Brunkhorst FM, Rea TD, Scherag A, Rubenfeld G, Kahn JM, Shankar-Hari M, Singer M and others. 2016. Assessment of Clinical Criteria for Sepsis: For the Third International Consensus Definitions for Sepsis and Septic Shock (Sepsis-3). JAMA 315:762-74.

Siddiqi N, House AO, Holmes JD. 2006. Occurrence and outcome of delirium in medical in-patients: a systematic literature review. Age Ageing 35:350-64.

Singer M, Deutschman CS, Seymour CW, Shankar-Hari M, Annane D, Bauer M, Bellomo R, Bernard GR, Chiche JD, Coopersmith CM and others. 2016. The Third International Consensus Definitions for Sepsis and Septic Shock (Sepsis-3). JAMA 315:801-10.

Soares MP, Gozzelino R, Weis S. 2014. Tissue damage control in disease tolerance. Trends Immunol 35:483-94.

Sonneville R, Verdonk F, Rauturier C, Klein IF, Wolff M, Annane D, Chretien F, Sharshar T. 2013. Understanding brain dysfunction in sepsis. Ann Intensive Care 3:15.

Soreide K. 2014. Clinical and translational aspects of hypothermia in major trauma patients: from pathophysiology to prevention, prognosis and potential preservation. Injury 45:647-54.

Stearns-Kurosawa DJ, Osuchowski MF, Valentine C, Kurosawa S, Remick DG. 2011. The pathogenesis of sepsis. Annu Rev Pathol 6:19-48.

Stephens LR, Eguinoa A, Erdjument-Bromage H, Lui M, Cooke F, Coadwell J, Smrcka AS, Thelen M, Cadwallader K, Tempst P and others. 1997. The G beta gamma sensitivity of a PI3K is dependent upon a tightly associated adaptor, p101. Cell 89:105-14.

Stoyanov B, Volinia S, Hanck T, Rubio I, Loubtchenkov M, Malek D, Stoyanova S, Vanhaesebroeck B, Dhand R, Nurnberg B and others. 1995. Cloning and characterization of a G protein-activated human phosphoinositide-3 kinase. Science 269:690-3.

Sun SF, Pan QZ, Hui X, Zhang BL, Wu HM, Li H, Xu W, Zhang Q, Li JY, Deng XM and others. 2008. Stronger in vitro phagocytosis by monocytes-macrophages is indicative of greater pathogen clearance and antibody levels in vivo. Poult Sci 87:1725-33.

Swoap SJ. 2008. The pharmacology and molecular mechanisms underlying temperature regulation and torpor. Biochem Pharmacol 76:817-24.

Szentirmai E, Krueger JM. 2014. Sickness behaviour after lipopolysaccharide treatment in ghrelin deficient mice. Brain Behav Immun 36:200-6.

Tauber SC, Eiffert H, Bruck W, Nau R. 2017. Septic encephalopathy and septic encephalitis. Expert Rev Anti Infect Ther 15:121-132.

Thomas D, Powell JA, Green BD, Barry EF, Ma Y, Woodcock J, Fitter S, Zannettino AC, Pitson SM, Hughes TP and others. 2013. Protein kinase activity of phosphoinositide 3-kinase regulates cytokine-dependent cell survival. PLoS Biol 11:e1001515.

van der Poll T, Opal SM. 2008. Host-pathogen interactions in sepsis. Lancet Infect Dis 8:32-43.

Vanhaesebroeck B, Guillermet-Guibert J, Graupera M, Bilanges B. 2010. The emerging mechanisms of isoform-specific PI3K signalling. Nat Rev Mol Cell Biol 11:329-41.

Vanhaesebroeck B, Leevers SJ, Panayotou G, Waterfield MD. 1997. Phosphoinositide 3-kinases: a conserved family of signal transducers. Trends Biochem Sci 22:267-72.

Verma S, Nakaoke R, Dohgu S, Banks WA. 2006. Release of cytokines by brain endothelial cells: A polarized response to lipopolysaccharide. Brain Behav Immun 20:449-55.

Voloboueva LA, Emery JF, Sun X, Giffard RG. 2013. Inflammatory response of microglial BV-2 cells includes a glycolytic shift and is modulated by mitochondrial glucose-regulated protein 75/mortalin. FEBS Lett 587:756-62.

Waage A, Halstensen A, Espevik T. 1987. Association between tumour necrosis factor in serum and fatal outcome in patients with meningococcal disease. Lancet 1:355-7.

West GB, Brown JH, Enquist BJ. 1997. A general model for the origin of allometric scaling laws in biology. Science 276:122-6.

Wetzker R, Rommel C. 2004. Phosphoinositide 3-kinases as targets for therapeutic intervention. Curr Pharm Des 10:1915-22.

Widmann CN, Heneka MT. 2014. Long-term cerebral consequences of sepsis. Lancet Neurol 13:630-6.

Wolf SA, Boddeke HW, Kettenmann H. 2017. Microglia in Physiology and Disease. Annu Rev Physiol 79:619-643.

Wymann MP, Solinas G. 2013. Inhibition of phosphoinositide 3-kinase gamma attenuates inflammation, obesity, and cardiovascular risk factors. Ann N Y Acad Sci 1280:44-7.

Yenari MA, Han HS. 2012. Neuroprotective mechanisms of hypothermia in brain ischaemia. Nat Rev Neurosci 13:267-78.

Young GB, Bolton CF, Austin TW, Archibald YM, Gonder J, Wells GA. 1990. The encephalopathy associated with septic illness. Clin Invest Med 13:297-304.

Young P, Saxena M, Bellomo R, Freebairn R, Hammond N, van Haren F, Holliday M, Henderson S, Mackle D, McArthur C and others. 2015. Acetaminophen for Fever in Critically Ill Patients with Suspected Infection. N Engl J Med 373:2215-24.

Young PJ, Saxena M, Beasley R, Bellomo R, Bailey M, Pilcher D, Finfer S, Harrison D, Myburgh J, Rowan K. 2012. Early peak temperature and mortality in critically ill patients with or without infection. Intensive Care Med 38:437-444.

Zhang F, Vadakkan KI, Kim SS, Wu LJ, Shang Y, Zhuo M. 2008. Selective activation of microglia in spinal cord but not higher cortical regions following nerve injury in adult mouse. Mol Pain 4:15.

Zhang LN, Wang XT, Ai YH, Guo QL, Huang L, Liu ZY, Yao B. 2012. Epidemiological features and risk factors of sepsis-associated encephalopathy in intensive care unit patients: 2008-2011. Chin Med J (Engl) 125:828-31.

Publications

Lang GP, Ndongson-Dongmo B, Lajqi T, Brodhun M, Marx C, Han YY, Wang Z-Q, Wetzker R, Bauer R. subm. Reduced ambient temperature enhances inflammation-induced encephalopathy in endotoxemic mice - Role of phosphoinositide 3-kinase gamma. *Journal of Neuroinflammation* (under revision)

Ndongson-Dongmo B*, **Lang GP***, Mece O, Hechaichi N, Lajqi T, Hoyer D, Brodhun M, Heller R, Wetzker R, Levy FO, Bauer R. Reduced ambient temperature exacerbates SIRS-induced cardiac autonomic dysregulation and myocardial dysfunction in mice. *Basic Research in Cardiology* (under revision)

Han YY*, Mora J*, Putyrski M, Huard A, da Silva P, Scholz A, Elwakeel E, **Lang GP**, Scholz T, Schmid T, de Bruin N, Billuart P, Sala C, Burkhardt H, Parnham M, Ernst A, Brüne B, and Weigert A. IL-38 restricts skin inflammation and anti-tumor immunity by limiting IL-17 production from γδ T cells through IL1RAPL1. *Cell reports* (under revision)

* Authors contributed equally to the work

Ehrenwörtliche Erklärung

Hiermit erkläre ich, dass mir die Promotionsordnung der Fakultät für Biowissenschaften der Friedrich-Schiller-Universität bekannt ist,

ich die Dissertation selbst angefertigt habe und alle von mir benutzten Hilfsmittel, persönlichen Mitteilungen und Quellen in meiner Arbeit angegeben sind,

mich folgende Personen bei der Auswahl und Auswertung des Materials sowie bei der Herstellung des Manuskripts unterstützt haben:

PhD Bernardin Ndongson-Dongmo: Durchführung von Tierexperimenten,

MTA Rose-Maria Zimmer: Unterstützung bei der Hirnpräparation, Histologie und Immunhistochemie

Mag. Trim Lajqi: Unterstützung bei Zellkultur-Arbeiten, Durchführung von PCR- und Elisa-Techniken

Prof. Dr. Reinhard Bauer und Prof. Dr. Reinhard Wetzker: Diskussion und Interpretation der Ergebnisse;

Prof. Dr. Reinhard Bauer: Redigieren der Dissertation;

die Hilfe eines Promotionsberaters nicht in Anspruch genommen wurde und dass Dritte weder unmittelbar noch mittelbar geldwerte Leistungen von mir für Arbeiten erhalten haben, die im Zusammenhang mit dem Inhalt der vorgelegten Dissertation stehen,

dass ich die Dissertation noch nicht als Prüfungsarbeit für eine staatliche oder andere wissenschaftliche Prüfung eingereicht habe und

dass ich die gleiche, eine in wesentlichen Teilen ähnliche oder eine andere Abhandlung nicht bei einer anderen Hochschule als Dissertation eingereicht habe.

Unterschrift des Verfassers

Acknowledgements